IEEE Access
Multidisciplinary : Rapid Review : Open Access Journal

Received November 23, 2021, accepted December 20, 2021, date of publication December 22, 2021, date of current version January 4, 2022.

Digital Object Identifier 10.1109/ACCESS.2021.3137719

A New Immersion and Invariance Control and Stable Deep Learning Fuzzy Approach for Power/Voltage Control Problem

MOHAMMAD HOSEIN SABZALIAN[1], KHALID A. ALATTAS[2], (Member, IEEE), MAURICIO AREDES[1], (Senior Member, IEEE), ABDULLAH K. ALANAZI[3], HALA M. ABO-DIEF[3], ARDASHIR MOHAMMADZADEH[4], SALEH MOBAYEN[5], (Senior Member, IEEE), BRUNO WANDERLEY FRANÇA[6], (Member, IEEE), AND AFEF FEKIH[7], (Senior Member, IEEE)

[1]Laboratory of Power Electronics and Medium Voltage Applications (LEMT), Alberto Luiz Coimbra Institute for Graduate Studies and Research in Engineering (COPPE), Federal University of Rio de Janeiro (UFRJ), Rio de Janeiro 21941-594, Brazil
[2]Department of Computer Science and Artificial Intelligence, College of Computer Science and Engineering, University of Jeddah, Jeddah 23890, Saudi Arabia
[3]Department of Chemistry, Collage of Science, Taif University, Taif 21944, Saudi Arabia
[4]Institute of Research and Development, Duy Tan University, Da Nang 550000, Vietnam
[5]Future Technology Research Center, National Yunlin University of Science and Technology, Douliu 64002, Taiwan
[6]Electrical Engineering Department, Fluminense Federal University, Niterói 24210-240, Brazil
[7]Department of Electrical and Computer Engineering, University of Louisiana at Lafayette, Lafayette, LA 70504, USA

Corresponding authors: Ardashir Mohammadzadeh (a.mzadeh@ieee.org) and Saleh Mobayen (mobayens@yuntech.edu.tw)

This work was supported by the Taif University Researchers Supporting Project under Grant TURSP-2020/266 of Taif University, Taif, Saudi Arabia; and in part by the Brazilian Agency CAPES.

ABSTRACT Background: The use of renewable energies is extended due to their valuable features such as abundant and clarity. The microgrids that include the renewable energies are widely used in various applications such as power supplying of remote areas, increasing the network reliability, reducing the greenhouse gas emission, reducing the consumption demand, eliminating the consumption peaks, and so on. But, energy management in the these systems in an challenging problem. Because, there are some natural perturbations such as variation output load, grid-side faults and changes of irradiation and temperature. Aim and Objective: The problem is to design a controller to regulate the output voltage/energy under aforementioned disturbances. Methods: The paper presents a new approach for energy management in Photovoltaic (PV)/Battery/Fuel Cells (FC) systems. The uncertainties are compensated by the new optimization rules based on Immersion and Invariance (I&I) theorem and proposed deep learning type-2 fuzzy logic compensator (T2FLC). The objective function of T2FLC is to minimize the tracking error in presence of perturbations. The adaptation rules are derived such that the I&I stabilization criterions are satisfied. Both rules and fuzzy sets (FSs) of T2FLCs are optimized by guaranteed stability rules to tackle the effect of perturbations and estimation errors. Results and Discussion: It is shown that a well voltage/energy regulation performance is achieved under variation of temperature, suddenly changes of load and variation of irradiation. A comparison with similar controllers demonstrates the superiority of the suggested approach. Conclusion: The suggested regulator do not depend on the mathematical models, and results in good accuracy under difficult conditions, then it can be used in various applications.

INDEX TERMS Energy management, immersion and invariance, deep learning, fuzzy systems, voltage control, stability.

I. INTRODUCTION

The energy management in microgrids including renewable energies has became one of the interesting topics in past decade. The dynamics of the hybrid systems that contains PVs, FCs and batteries are always disturbed by nature factors such as variation output load, grid-side faults and changes of irradiation and temperature. The designing of strong control systems to kept output voltage and power in a desired level is one of the challenging problems [1]–[4].

Many control systems have been presented for power and voltage regulation. For example, the power fluctuation is

The associate editor coordinating the review of this manuscript and approving it for publication was Behnam Mohammadi-Ivatloo.

studied in [5], and a balancing controller is proposed. In [6], a predictive controller is presented to cope with the effect of variation of electricity tariff and irradiation. In [7], an energy management technique is designed by battery charging control scheme to reduce the operating cost. In [8], the dynamics of PV panels and batteries are modeled and then a control system is suggested for stabilizing output voltage. In [9], a multi-objective controller is developed to regulate output voltage under nonlinear output load. The mode-triggered droop controller is designed in [10] for energy management, and its energy distribution capability is examined in various conditions. In [11], a multifunctional controller is developed, the problem of harmonics mitigation is investigated, and improvement of the power quality is shown. In [12], a distributed control method is suggested for power regulation, and robustness against time delays is studied. The coordinated control scheme is developed in [13], to improve the battery life.

To tackle the effect of perturbations and dynamic uncertainties, some fuzzy and neural controllers have been developed [14]. For example, a fuzzy logic controller (FLC) is introduced in [15], and the superiority of FLC is shown under fluctuation of PV power. In [16], the fluctuation of the output load is taken to account, and the efficiency improvement by FLC is shown. In [17], a FLC is designed to make an energy balance between PV and FC, and the parameters of FLC are optimized by genetic algorithm. The energy management is studied by cuckoo algorithm in [18], to compensate PV power shortage in necessary times. In [19], a FLC is proposed to handle the uncertain dynamics of PV and FCs, and by comparison with conventional controllers the good proficiency of FLCs is demonstrated. The effect of fast load variation is studied in [20] by designing an FLC, and it is shown that energy consumption is decreased about 19.6%. In [19], the dynamic perturbation by variation of temperature is studied and an FLC is designed. The PV and FC dynamic modeling is studied in [21], and a simple FLC is suggested for application in electric vehicles. The optimization of hydrogen production is investigated in [22] by FLC, and the superiority of FLCs in term of less required expertise is discussed. Compassion of various approaches in reviewed in [23].

Recently, the better capability of type-2 FLCs and deep learning algorithms have been shown in various problems such as internet of things [24], wireless sensor networks [25], robotics [26], clustering problems [27], power systems [28], electrical vehicles [29], control systems [30], and so on. However, this type of FLCs with guaranteed stability have been rarely studied. In [31], a high-order FLC is presented for estimation of uncertainties in PV and battery dynamics. In [32], a T2FLC is developed to cope with irradiation fluctuations. The main drawback of aforementioned studies is that, only rule parameters are optimized, and the antecedent parameters are neglected. Also, the online stability guarantee in the most of presented controllers needs more investigation. In current paper, we present the novel adaptation laws for uncertain parameters based on I&I theorem. The effect of disturbances such as variation of temperature, fluctuation of irradiation and changes of output load are compensated by the suggested deep learning T2FLC by guaranteed stability. The main contributions and the advantages of the suggested method are:

- The novel adaptation laws are presented for uncertain parameters based on I&I theorem.
- The effect of disturbances such as variation of temperature, fluctuation of irradiation and changes of output load are compensated.
- A deep learning T2FLC by guaranteed stability is presented.
- Both rules and FS parameters are optimized.
- The superiority of the designed method is examined under various conditions and comparison with other conventional approaches.

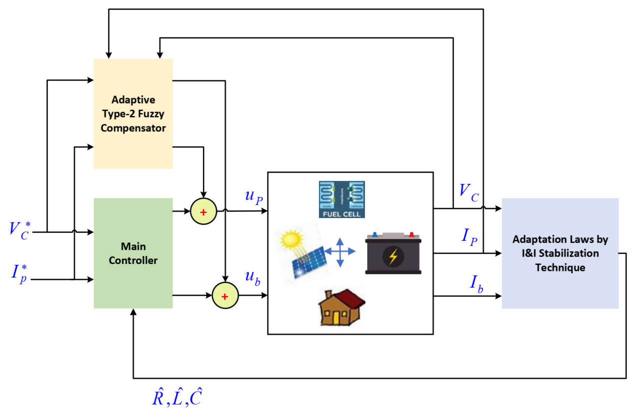

FIGURE 1. The control block diagram.

II. PROBLEM FORMULATION

A. GENERAL VIEW

The designed control scheme is depicted in Fig. 1. The dynamics are considered to be uncertain. The adaptation rules are derived by the I&I stabilization approach. The perturbations are compensated by the suggested T2FLC. As shown in Fig. 1, unlike the conventional studies [33]–[35], the adaptation laws are derived form I&I stabilization approach. The main uncertain parameters are estimated by the extracted adaptation laws. Then, the estimation error is taken into account, and a T2FLC is designed. The rules of T2FLC are optimized such that the effect of estimation error is eliminated.

B. FUEL CELL

Today, the role of new and renewable energy sources in the production of electricity is not hidden from anyone. In addition to solar, wind, geothermal and biomass energy, fuel cell energy has also become very important. A fuel cell (FC) is a device that generates electricity through a chemical reaction. All fuel cells have two electrical poles (electrodes) called anodes and cathodes. In fact, chemical reactions take place

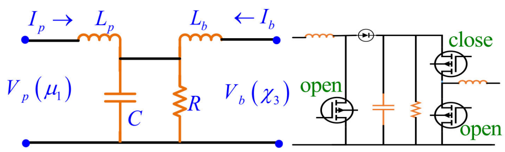

FIGURE 2. Boost convertor: switching mode #1.

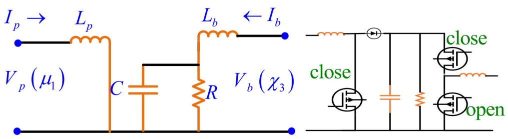

FIGURE 3. Boost convertor: switching mode #2.

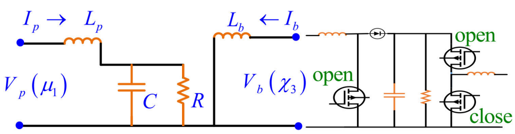

FIGURE 4. Boost convertor: switching mode #3.

in these electrodes, leading to the generation of electricity. In addition, each FC has an electrolyte and a catalyst; The role of the electrolyte is to move charged particles between the electrodes, while the catalyst speeds up the reactions at the electrodes. Although hydrogen is the main fuel, oxygen is also needed to form the reaction. One of the biggest superiorities of an FC is that it generates electricity with the least amount of pollution. In fact, most of the oxygen and hydrogen entering the cell is eventually released as a harmless by-product, water. An FC generates a very small amount of direct current, which is why a large number of cells are used to generate electricity in large batches called stacks. The dynamics of FC are given as:

$$\begin{aligned} V_{FC} &= -\iota I_{FC} \\ &\quad + \left(\ln\left(\xi_{H_2}\cdot\xi_{O_2}^{0.5}/\xi_{H_2O}\right)\cdot(T\Re/2F)+E_0\right)N_0 \quad (1)\\ Q_{H_2} &= 2I_{FC}\tau_\iota/\left[U_{opt}\left(\kappa_f\cdot s+1\right)\right] \quad (2)\\ Q_{O_2^{in}} &= \frac{Q_{H_2^{in}}}{\iota_{HO}} \quad (3)\\ \xi_{H_2} &= \frac{Q_{H_2^{in}}-2\tau_\iota I_{FC}}{k_{H_2}\left(s\kappa_{H_2}+1\right)} \quad (4)\\ \xi_{O_2} &= \left(Q_{O_2^{in}}-\tau_\iota I_{FC}\right)/k_{O_2}\left(s\kappa_{O_2}+1\right) \quad (5)\\ \xi_{H_2O} &= 2\tau_\iota I_{FC}/\left[\left(s\cdot\kappa_{H_2O}+1\right)\cdot k_{H_2O}\right] \quad (6) \end{aligned}$$

where, the parameters and variables are described Tables 3- 4, in Appendix.

C. CONVERTERS

The switching mechanism between units is constructed by the use of Boost converters. As shown in Figs. 2-5, we have four switching modes. By averaging the four state space models,

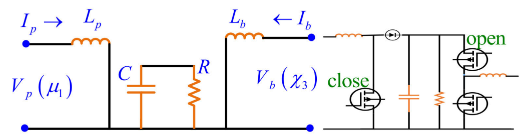

FIGURE 5. Boost convertor: switching mode #4.

we obtain:

$$\begin{aligned} \dot{\mu}_1 &= \left(-\mu_2+V_p\left(\mu_1\right)+\mu_2u_p\right)/L_p \\ \dot{\mu}_2 &= \frac{1}{C}\left(\mu_1-\mu_2/R+\mu_3u_b-\mu_1u_p\right) \\ \dot{\mu}_3 &= \left(-\mu_2u_b+V_b\left(\mu_3\right)\right)/L_b \quad (7) \end{aligned}$$

where, I_p/I_b denotes PV/battery currents and V_c represents the load voltage.

D. PV MODELING

By the use of single-diode method [36], the dynamics of PV are given as:

$$\begin{aligned} i_{ph} &= s\left(k_i\left(T-T_\iota\right)+i_{sc}\right) \quad (8)\\ I_p &= G\cdot I_{phg} \\ &\quad -\exp\left(Q\left(V_p+I_p\Re_{sg}\right)/nTk_b-1\right)i_o \\ &\quad -\left(I_p\Re_{sg}+V_p\right)/\Re_{shg} \quad (9)\\ i_0 &= e^{\left[QE_g\left(\frac{1}{T_\iota+273}-\frac{1}{T+273}\right)/k_bA\right]}\left(\frac{T+273}{T_\iota+273}\right)^3 i_\iota \quad (10) \end{aligned}$$

where, all parameters descriptions are given in Table 5 in Appendix.

E. BATTERY MODELING

The dynamics of battery are written as [36]:

$$\begin{aligned} E\left(t\right) &= -\int \alpha V_{boc}I_b+E_{Loss}dt \quad (11)\\ \alpha &= \begin{cases}\alpha_1\; I_b\geq 0\\ \alpha_2\; I_b<0,\end{cases} \quad (12)\\ V_b &= V_{boc}-I_b\cdot\iota_b \quad (13)\\ SoC\left(t\right) &= E\left(t\right)/E_{Max} \quad (14) \end{aligned}$$

The parameter descriptions are given in Table 6, in Appendix.

III. TYP-2 FLC

The type-2 FLSs are the generalization of type-1 counterparts which can support more level of uncertainties. A type-2 fuzzy set has three dimensions, which its third dimension represents the secondary membership. In other words, in type-2 fuzzy sets, the memberships are not crisp values but they are fuzzy numbers. As mentioned earlier, in the power/voltage control problem of microgrids, we face a large number of perturbations, and we need a strong tool to tackle the effect of various disturbances such as dynamic uncertainties, estimation errors of adaptation rules, variation of output load, grid-side faults and changes of irradiation and temperature. Then we formulate a type-2 fuzzy compensator. The structure is given

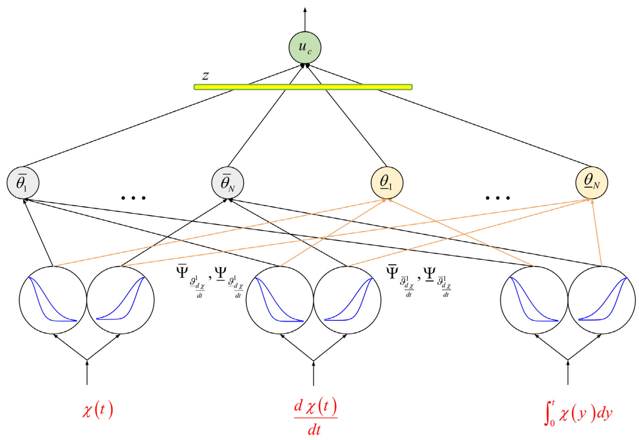

FIGURE 6. **Type-2 fuzzy compensator.**

in Fig. 6. The computations are as: 1) The inputs are tracking error ($\chi(t)$), derivative of tracking error $\frac{d\chi(t)}{dt}$ and integral of tracking error $\int_0^t \chi(y)\,dy$.

2) The memberships for are obtained as:

$$\bar{\Psi}_{\bar{\vartheta}_\chi}(\chi(t)) = \exp\left(-\frac{\left(\chi(t) - M_{\bar{\vartheta}_\chi}\right)^2}{\bar{\sigma}^2_{\bar{\vartheta}_\chi}}\right)$$

$$\underline{\Psi}_{\bar{\vartheta}_\chi}(\chi(t)) = \exp\left(-\frac{\left(\chi(t) - M_{\bar{\vartheta}_\chi}\right)^2}{\underline{\sigma}^2_{\bar{\vartheta}_\chi}}\right) \tag{15}$$

$$\bar{\Psi}_{\underline{\vartheta}_\chi}(\chi(t)) = \exp\left(-\frac{\left(\chi(t) - M_{\underline{\vartheta}_\chi}\right)^2}{\bar{\sigma}^2_{\underline{\vartheta}_\chi}}\right)$$

$$\underline{\Psi}_{\underline{\vartheta}_\chi}(\chi(t)) = \exp\left(-\frac{\left(\chi(t) - M_{\underline{\vartheta}_\chi}\right)^2}{\underline{\sigma}^2_{\underline{\vartheta}_\chi}}\right) \tag{16}$$

where, $M_{\bar{\vartheta}_\chi}$ and $M_{\underline{\vartheta}_\chi}$ are the centers of MFs $\bar{\vartheta}_\chi$ and $\underline{\vartheta}_\chi$, respectively. $\bar{\sigma}_{\bar{\vartheta}_\chi}/\underline{\sigma}_{\bar{\vartheta}_\chi}$ is the upper/lower width of $\bar{\vartheta}_\chi$. $\bar{\sigma}_{\underline{\vartheta}_\chi}/\underline{\sigma}_{\underline{\vartheta}_\chi}$ is the upper/lower width of $\underline{\vartheta}_\chi$. Similarly for the input $\frac{d\chi}{dt}$ we have:

$$\bar{\Psi}_{\bar{\vartheta}_{\frac{d\chi}{dt}}}\left(\frac{d\chi}{dt}(t)\right) = \exp\left(-\frac{\left(\frac{d\chi}{dt}(t) - M_{\bar{\vartheta}_{\frac{d\chi}{dt}}}\right)^2}{\bar{\sigma}^2_{\bar{\vartheta}_{\frac{d\chi}{dt}}}}\right)$$

$$\underline{\Psi}_{\bar{\vartheta}_{\frac{d\chi}{dt}}}\left(\frac{d\chi}{dt}(t)\right) = \exp\left(-\frac{\left(\frac{d\chi}{dt}(t) - M_{\bar{\vartheta}_{\frac{d\chi}{dt}}}\right)^2}{\underline{\sigma}^2_{\bar{\vartheta}_{\frac{d\chi}{dt}}}}\right) \tag{17}$$

$$\bar{\Psi}_{\underline{\vartheta}_{\frac{d\chi}{dt}}}\left(\frac{d\chi}{dt}(t)\right) = \exp\left(-\frac{\left(\frac{d\chi}{dt}(t) - M_{\underline{\vartheta}_{\frac{d\chi}{dt}}}\right)^2}{\bar{\sigma}^2_{\underline{\vartheta}_{\frac{d\chi}{dt}}}}\right)$$

$$\underline{\Psi}_{\underline{\vartheta}_{\frac{d\chi}{dt}}}\left(\frac{d\chi}{dt}(t)\right) = \exp\left(-\frac{\left(\frac{d\chi}{dt}(t) - M_{\underline{\vartheta}_{\frac{d\chi}{dt}}}\right)^2}{\underline{\sigma}^2_{\underline{\vartheta}_{\frac{d\chi}{dt}}}}\right) \tag{18}$$

where, $M_{\bar{\vartheta}_{\frac{d\chi}{dt}}}$ and $M_{\underline{\vartheta}_{\frac{d\chi}{dt}}}$ are the centers of MFs $\bar{\vartheta}_{\frac{d\chi}{dt}}$ and $\underline{\vartheta}_{\frac{d\chi}{dt}}$, respectively. $\bar{\sigma}_{\bar{\vartheta}_{\frac{d\chi}{dt}}}$ and $\underline{\sigma}_{\bar{\vartheta}_{\frac{d\chi}{dt}}}$ are the upper and lower width of $\bar{\vartheta}_{\frac{d\chi}{dt}}$. $\bar{\sigma}_{\underline{\vartheta}_{\frac{d\chi}{dt}}}/\underline{\sigma}_{\underline{\vartheta}_{\frac{d\chi}{dt}}}$ is the upper/lower width of $\underline{\vartheta}_{\frac{d\chi}{dt}}$. Finally, for input $\int_0^t \chi(y)\,dy$, the memberships are:

$$\bar{\Psi}_{\bar{\vartheta}_{\int_0^t \chi(y)dy}}\left(\int_0^t \chi(y)\,dy\right) = \exp\left(-\frac{\left(\int_0^t \chi(y)\,dy(t) - M_{\bar{\vartheta}_{\int_0^t \chi(y)dy}}\right)^2}{\bar{\sigma}^2_{\bar{\vartheta}_{\int_0^t \chi(y)dy}}}\right)$$

$$\underline{\Psi}_{\bar{\vartheta}_{\int_0^t \chi(y)dy}}\left(\int_0^t \chi(y)\,dy\right) = \exp\left(-\frac{\left(\int_0^t \chi(y)\,dy(t) - M_{\bar{\vartheta}_{\int_0^t \chi(y)dy}}\right)^2}{\underline{\sigma}^2_{\bar{\vartheta}_{\int_0^t \chi(y)dy}}}\right) \tag{19}$$

$$\bar{\Psi}_{\underline{\vartheta}_{\int_0^t \chi(y)dy}}\left(\int_0^t \chi(y)\,dy\right) = \exp\left(-\frac{\left(\int_0^t \chi(y)\,dy(t) - M_{\underline{\vartheta}_{\int_0^t \chi(y)dy}}\right)^2}{\bar{\sigma}^2_{\underline{\vartheta}_{\int_0^t \chi(y)dy}}}\right)$$

$$\underline{\Psi}_{\underline{\vartheta}_{\int_0^t \chi(y)dy}}\left(\int_0^t \chi(y)\,dy\right) = \exp\left(-\frac{\left(\int_0^t \chi(y)\,dy(t) - M_{\underline{\vartheta}_{\int_0^t \chi(y)dy}}\right)^2}{\underline{\sigma}^2_{\underline{\vartheta}_{\int_0^t \chi(\omega)d\omega}}}\right) \tag{20}$$

where, $M_{\bar{\vartheta}_{\int_0^t \chi(\omega)d\omega}}$ and $M_{\underline{\vartheta}_{\int_0^t \chi(\omega)d\omega}}$ are the centers of MFs $\bar{\vartheta}_{\int_0^t \chi(\omega)d\omega}$ and $\underline{\vartheta}_{\int_0^t \chi(\omega)d\omega}$, respectively. $\bar{\sigma}_{\bar{\vartheta}_{\int_0^t \chi(\omega)d\omega}}/\underline{\sigma}_{\bar{\vartheta}_{\int_0^t \chi(\omega)d\omega}}$ is the upper/lower width of $\bar{\vartheta}_{\int_0^t \chi(\omega)d\omega}$. $\bar{\sigma}_{\underline{\vartheta}_{\int_0^t \chi(\omega)d\omega}}/\underline{\sigma}_{\underline{\vartheta}_{\int_0^t \chi(\omega)d\omega}}$ is the upper/lower width of $\underline{\vartheta}_{\int_0^t \chi(\omega)d\omega}$.

3) The rules firing are obtained as:

$$\bar{\theta}_1 = \bar{\Psi}_{\bar{\vartheta}_\chi}(\chi(t)) \cdot \bar{\Psi}_{\bar{\vartheta}_{\frac{d\chi}{dt}}}\left(\frac{d\chi}{dt}(t)\right) \cdot \bar{\Psi}_{\bar{\vartheta}_{\int_0^t \chi(y)dy}}\left(\int_0^t \chi(y)\,dy\right)$$

$$\bar{\theta}_2 = \bar{\Psi}_{\bar{\vartheta}_\chi}(\chi(t)) \cdot \bar{\Psi}_{\bar{\vartheta}_{\frac{d\chi}{dt}}}\left(\frac{d\chi}{dt}(t)\right) \cdot \bar{\Psi}_{\underline{\vartheta}_{\int_0^t \chi(y)dy}}\left(\int_0^t \chi(y)\,dy\right)$$

$$\begin{aligned}
&\bar{\theta}_3\\
&=\bar{\Psi}_{\bar{\vartheta}_\chi}\left(\chi\left(t\right)\right)\cdot\bar{\Psi}_{\underline{\vartheta}_{\frac{d\chi}{dt}}}\left(\frac{d\chi}{dt}\left(t\right)\right)\cdot\bar{\Psi}_{\bar{\vartheta}_{\int_0^t\chi(y)dy}}\left(\int_0^t\chi\left(y\right)dy\right)\\
&\bar{\theta}_4\\
&=\bar{\Psi}_{\bar{\vartheta}_\chi}\left(\chi\left(t\right)\right)\cdot\bar{\Psi}_{\underline{\vartheta}_{\frac{d\chi}{dt}}}\left(\frac{d\chi}{dt}\left(t\right)\right)\cdot\bar{\Psi}_{\underline{\vartheta}_{\int_0^t\chi(y)dy}}\left(\int_0^t\chi\left(y\right)dy\right)\\
&\bar{\theta}_5\\
&=\bar{\Psi}_{\underline{\vartheta}_\chi}\left(\chi\left(t\right)\right)\cdot\bar{\Psi}_{\bar{\vartheta}_{\frac{d\chi}{dt}}}\left(\frac{d\chi}{dt}\left(t\right)\right)\cdot\bar{\Psi}_{\bar{\vartheta}_{\int_0^t\chi(y)dy}}\left(\int_0^t\chi\left(y\right)dy\right)\\
&\bar{\theta}_6\\
&=\bar{\Psi}_{\underline{\vartheta}_\chi}\left(\chi\left(t\right)\right)\cdot\bar{\Psi}_{\bar{\vartheta}_{\frac{d\chi}{dt}}}\left(\frac{d\chi}{dt}\left(t\right)\right)\cdot\bar{\Psi}_{\underline{\vartheta}_{\int_0^t\chi(y)dy}}\left(\int_0^t\chi\left(y\right)dy\right)\\
&\bar{\theta}_7\\
&=\bar{\Psi}_{\underline{\vartheta}_\chi}\left(\chi\left(t\right)\right)\cdot\bar{\Psi}_{\underline{\vartheta}_{\frac{d\chi}{dt}}}\left(\frac{d\chi}{dt}\left(t\right)\right)\cdot\bar{\Psi}_{\bar{\vartheta}_{\int_0^t\chi(y)dy}}\left(\int_0^t\chi\left(y\right)dy\right)\\
&\bar{\theta}_8\\
&=\bar{\Psi}_{\underline{\vartheta}_\chi}\left(\chi\left(t\right)\right)\cdot\bar{\Psi}_{\underline{\vartheta}_{\frac{d\chi}{dt}}}\left(\frac{d\chi}{dt}\left(t\right)\right)\cdot\bar{\Psi}_{\underline{\vartheta}_{\int_0^t\chi(y)dy}}\left(\int_0^t\chi\left(y\right)dy\right)
\end{aligned}\tag{21}$$

$$\begin{aligned}
&\underline{\theta}_1\\
&=\underline{\Psi}_{\bar{\vartheta}_\chi}\left(\chi\left(t\right)\right)\cdot\underline{\Psi}_{\bar{\vartheta}_{\frac{d\chi}{dt}}}\left(\frac{d\chi}{dt}\left(t\right)\right)\cdot\underline{\Psi}_{\bar{\vartheta}_{\int_0^t\chi(y)dy}}\left(\int_0^t\chi\left(y\right)dy\right)\\
&\underline{\theta}_2\\
&=\underline{\Psi}_{\bar{\vartheta}_\chi}\left(\chi\left(t\right)\right)\cdot\underline{\Psi}_{\bar{\vartheta}_{\frac{d\chi}{dt}}}\left(\frac{d\chi}{dt}\left(t\right)\right)\cdot\underline{\Psi}_{\underline{\vartheta}_{\int_0^t\chi(y)dy}}\left(\int_0^t\chi\left(y\right)dy\right)\\
&\underline{\theta}_3\\
&=\underline{\Psi}_{\bar{\vartheta}_\chi}\left(\chi\left(t\right)\right)\cdot\underline{\Psi}_{\underline{\vartheta}_{\frac{d\chi}{dt}}}\left(\frac{d\chi}{dt}\left(t\right)\right)\cdot\underline{\Psi}_{\bar{\vartheta}_{\int_0^t\chi(y)dy}}\left(\int_0^t\chi\left(y\right)dy\right)\\
&\underline{\theta}_4\\
&=\underline{\Psi}_{\bar{\vartheta}_\chi}\left(\chi\left(t\right)\right)\cdot\underline{\Psi}_{\underline{\vartheta}_{\frac{d\chi}{dt}}}\left(\frac{d\chi}{dt}\left(t\right)\right)\cdot\underline{\Psi}_{\underline{\vartheta}_{\int_0^t\chi(y)dy}}\left(\int_0^t\chi\left(y\right)dy\right)\\
&\underline{\theta}_5\\
&=\underline{\Psi}_{\underline{\vartheta}_\chi}\left(\chi\left(t\right)\right)\cdot\underline{\Psi}_{\bar{\vartheta}_{\frac{d\chi}{dt}}}\left(\frac{d\chi}{dt}\left(t\right)\right)\cdot\underline{\Psi}_{\bar{\vartheta}_{\int_0^t\chi(y)dy}}\left(\int_0^t\chi\left(y\right)dy\right)\\
&\underline{\theta}_6\\
&=\underline{\Psi}_{\underline{\vartheta}_\chi}\left(\chi\left(t\right)\right)\cdot\underline{\Psi}_{\bar{\vartheta}_{\frac{d\chi}{dt}}}\left(\frac{d\chi}{dt}\left(t\right)\right)\cdot\underline{\Psi}_{\underline{\vartheta}_{\int_0^t\chi(y)dy}}\left(\int_0^t\chi\left(y\right)dy\right)\\
&\underline{\theta}_7\\
&=\underline{\Psi}_{\underline{\vartheta}_\chi}\left(\chi\left(t\right)\right)\cdot\underline{\Psi}_{\underline{\vartheta}_{\frac{d\chi}{dt}}}\left(\frac{d\chi}{dt}\left(t\right)\right)\cdot\underline{\Psi}_{\bar{\vartheta}_{\int_0^t\chi(y)dy}}\left(\int_0^t\chi\left(y\right)dy\right)\\
&\underline{\theta}_8\\
&=\underline{\Psi}_{\underline{\vartheta}_\chi}\left(\chi\left(t\right)\right)\cdot\underline{\Psi}_{\underline{\vartheta}_{\frac{d\chi}{dt}}}\left(\frac{d\chi}{dt}\left(t\right)\right)\cdot\underline{\Psi}_{\underline{\vartheta}_{\int_0^t\chi(y)dy}}\left(\int_0^t\chi\left(y\right)dy\right)
\end{aligned}\tag{22}$$

4) The output is computed as:

$$u_c\left(z|X\right)=\frac{\sum_{i=1}^{N}z_i\left(\bar{\theta}_i+\underline{\theta}_i\right)}{\sum_{i=1}^{N}\bar{\theta}_i+\underline{\theta}_i}\tag{23}$$

where, N represents number of rules and:

$$z^T=\left[z_1,\ldots,z_N\right]\tag{24}$$

$$X^T=\left[\chi\left(t\right),\frac{d\chi}{dt}\left(t\right),\int_0^t\chi\left(y\right)dy\right]\tag{25}$$

IV. I&I ADAPTATION LAWS

In this section the main tuning rules are presented and the stability is investigated. Unlike the most conventional studies, the tuning rules are extracted from I&I stability analysis. The tuning rules for uncertain parameters are considered such that all criteria of I&I theorem are satisfied. Following, the details are given in Theorem 1. Before, the presenting the Theorem 1, the main I&I Lemma is given as:

Lemma 1 (I&I Stabilization [37]): Consider the dynamics of under control plant as:

$$\dot{\mu}=F\left(\mu\right)+H\left(\mu\right)u\tag{26}$$

where, $F\left(\mu\right)$ and $H\left(\mu\right)$ are nonlinear functions with unknown parameters w and equilibrium point μ^*. The system (26) is I&I stabilizable, if there is α_1 and α_2 such that all trajectories of (27):

$$\begin{aligned}
\dot{x}&=F\left(\mu\right)+H\left(\mu\right)u\left(\mu,\hat{w}+\alpha_1\left(\mu\right)\right)\\
\frac{d\hat{w}}{dt}&=\alpha_2\left(\mu,\hat{w}\right)
\end{aligned}\tag{27}$$

are staying on:

$$\varphi=\left\{\left(\mu,w\right)|\hat{w}-w+\alpha_1\left(\mu\right)=0\right\}\tag{28}$$

Our results are given in the Theorem 1.

Theorem 1: By the controllers (29-30) and adaptation rules (31-33) the stability is ensured.

$$u_p=\frac{1}{\mu_2}\left[\left(\dot{r}_1+\lambda_1\chi_1\right)\left(\hat{L}_P+\eta\tilde{L}_P\left(\chi\right)\right)+\mu_2-V_p\left(\mu_1\right)\right]\tag{29}$$

$$\begin{aligned}
u_b=\frac{1}{\mu_3}&\left[\left(\dot{r}_2+\lambda_2\chi_2\right)\left(\hat{C}+\eta\tilde{C}\left(\chi\right)\right)-\mu_1\right.\\
&\left.+\mu_2/\left(\hat{R}+\eta\tilde{R}\left(\chi\right)\right)+\mu_1u_p\right]
\end{aligned}\tag{30}$$

$$\dot{\hat{L}}_P=\eta\frac{\partial\tilde{L}_P\left(\chi\right)}{\partial\chi_1}\lambda_1\chi_1+\eta\frac{\partial\tilde{L}_P\left(\chi\right)}{\partial\chi_2}\lambda_2\chi_2\tag{31}$$

$$\dot{\hat{R}}=\eta\frac{\partial\tilde{R}\left(\chi\right)}{\partial\chi_1}\lambda_1\chi_1+\eta\frac{\partial\tilde{R}\left(\chi\right)}{\partial\chi_2}\lambda_2\chi_2\tag{32}$$

$$\dot{\hat{C}}=\eta\frac{\partial\tilde{C}\left(\chi\right)}{\partial\chi_1}\lambda_1\chi_1+\eta\frac{\partial\tilde{C}\left(\chi\right)}{\partial\chi_2}\lambda_2\chi_2\tag{33}$$

where, r_i represents the reference signal for outputs μ_i and:

$$\frac{\partial\tilde{L}_P\left(\chi\right)}{\partial\chi_1}=\dot{r}_1+\lambda_1\chi_1\tag{34}$$

$$\frac{\partial\tilde{L}_P\left(\chi\right)}{\partial\chi_2}=0\tag{35}$$

$$\frac{\partial\tilde{R}\left(\chi\right)}{\partial\chi_1}=0\tag{36}$$

$$\frac{\partial \tilde{R}(\chi)}{\partial \chi_2} = -\left(\hat{R} + \eta \tilde{R}(\chi)\right) \tag{37}$$
$$\frac{\partial \tilde{C}(\chi)}{\partial \chi_1} = 0 \tag{38}$$
$$\frac{\partial \tilde{C}(\chi)}{\partial \chi_2} = \dot{r}_2 + \lambda_2 \chi_2 \tag{39}$$

where, λ_i and η are constant and $\chi_i\ i = 1, 2$ are defined as:

$$\begin{aligned} \chi_1 &\triangleq r_1 - \mu_1 \\ \chi_2 &\triangleq r_2 - \mu_2 \end{aligned} \tag{40}$$

Proof: The dynamics are estimated as:

$$\begin{aligned} \dot{\mu}_1 &= \left(-\mu_2 + V_p(\mu_1) + \mu_2 u_p\right)/\hat{L}_p \\ \dot{\mu}_2 &= \frac{1}{\hat{C}}\left(\mu_1 - \mu_2/\hat{R} + \mu_3 u_b - \mu_1 u_p\right) \\ \dot{\mu}_3 &= \left(-\mu_2 u_b + V_b(\mu_3)\right)/\hat{L}_b \end{aligned} \tag{41}$$

The reference dynamics are assumed to be:

$$\begin{aligned} \dot{\chi}_1 &= -\lambda_1 \chi_1 \\ \dot{\chi}_2 &= -\lambda_2 \chi_2 \end{aligned} \tag{42}$$

Time derivative of (40), gives:

$$\begin{aligned} \dot{\chi}_1 &= \dot{r}_1 - \dot{\mu}_1 \\ \dot{\chi}_2 &= \dot{r}_2 - \dot{\mu}_2 \end{aligned} \tag{43}$$

By substituting of $\dot{\mu}_i$, equation (43) becomes:

$$\begin{aligned} \dot{\chi}_1 &= \dot{r}_1 - \left(-\mu_2 + V_p(\mu_1) + \mu_2 u_p(\chi, L_p)\right)/L_p \\ \dot{\chi}_2 &= \dot{r}_2 - \frac{1}{C}\left(\mu_1 - \mu_2/R + \mu_3 u_b(\chi, C, R) - \mu_1 u_p\right) \end{aligned} \tag{44}$$

Considering Lemma 1, (44) is extended as:

$$\begin{aligned} \dot{\chi}_1 &= \dot{r}_1 \\ &\quad -\left(-\mu_2 + V_p(\mu_1) + \mu_2 u_p\left(\chi, \hat{L}_p + \eta \tilde{L}_p(\chi)\right)\right)/L_p \\ \dot{\chi}_2 &= \dot{r}_2 \\ &\quad -\frac{1}{C}\begin{pmatrix} \mu_1 - \mu_2/R + \\ \mu_3 u_b\left(\chi, \hat{C} + \eta \tilde{C}(\chi), \hat{R} + \eta \tilde{R}(\chi)\right) - \mu_1 u_p \end{pmatrix} \end{aligned} \tag{45}$$

where,

$$\dot{\hat{L}}_p = \psi_L\left(\chi, \hat{L}_p\right) \tag{46}$$
$$\dot{\hat{R}} = \psi_R\left(\chi, \hat{R}\right) \tag{47}$$
$$\dot{\hat{C}} = \psi_C\left(\chi, \hat{C}\right) \tag{48}$$
$$\chi = [\chi_1, \chi_2]^T \tag{49}$$

where, $\hat{L}_P$, $\hat{R}$ and $\hat{C}$ are the estimation of L_P, R and C. The system (45), is I&I stabilizable if there exist $\tilde{L}_p$, $\tilde{R}$, $\tilde{C}$, ψ_R, ψ_{L_P} and ψ_C, such that:

$$\varphi_L = \left\{(\chi, L_P) \in \Re^{n+1} | \hat{L}_P + \eta \tilde{L}_P(\chi) - \hat{L}_P = 0\right\} \tag{50}$$
$$\varphi_R = \left\{(\chi, R) \in \Re^{n+1} | \hat{R} + \eta \tilde{R}(\chi) - R = 0\right\} \tag{51}$$
$$\varphi_C = \left\{(\chi, C) \in \Re^{n+1} | \hat{C} + \eta \tilde{C}(\chi) - C = 0\right\} \tag{52}$$

where, $n = 2$ and η is a constant. To satisfy (50-52), the stability of the following errors should be ensured:

$$e_P = \hat{L}_P + \eta \tilde{L}_P(\chi) - L_P \tag{53}$$
$$e_R = \hat{R} + \eta \tilde{R}(\chi) - R \tag{54}$$
$$e_C = \hat{C} + \eta \tilde{C}(\chi) - C \tag{55}$$

Form (53-55), the equation (44) is rewritten as:

$$\begin{aligned} \dot{\chi}_1 &= \dot{r}_1 \\ &\quad -\left(-\mu_2 + V_p(\mu_1) + \mu_2 u_p\right)/\left(\hat{L}_P + \eta \tilde{L}_P(\chi) - e_P\right) \\ \dot{\chi}_2 &= \dot{r}_2 - \frac{1}{\left(\hat{C} + \eta \tilde{C}(\chi) - e_C\right)} \\ &\quad \times \begin{pmatrix} \mu_1 - \mu_2/\left(\hat{R} + \eta \tilde{R}(\chi) - e_R\right) \\ +\mu_3 u_b - \mu_1 u_p \end{pmatrix} \end{aligned} \tag{56}$$

By applying controllers (29-30) on (56), we have:

$$\dot{\chi}_1 = \dot{r}_1 - \frac{(\dot{r}_1 + \lambda_1 \chi_1)\left(\hat{L}_P + \eta \tilde{L}_P(\chi)\right)}{\left(\hat{L}_P + \eta \tilde{L}_P(\chi) - e_P\right)} \tag{57}$$

$$\begin{aligned} \dot{\chi}_2 &= \dot{r}_2 \\ &\quad - \frac{1}{\left(\hat{C} + \eta \tilde{C}(\chi) - e_C\right)}\left[\begin{matrix} -\mu_2/\left(\hat{R} + \eta \tilde{R}(\chi) - e_R\right) \\ +\mu_2/\left(\hat{R} + \eta \tilde{R}(\chi)\right) \\ +(\dot{r}_2 + \lambda_2 \chi_2)\left(\hat{C} + \eta \tilde{C}(\chi)\right) \end{matrix}\right] \end{aligned} \tag{58}$$

Equations (57-58), can be simplified as:

$$\dot{\chi}_1 = \dot{r}_1 - (\dot{r}_1 + \lambda_1 \chi_1)\left[1 + \frac{e_P}{\hat{L}_P + \eta \tilde{L}_P(\chi) - e_P}\right] \tag{59}$$

$$\begin{aligned} \dot{\chi}_2 &= \dot{r}_2 \\ &\quad - \frac{1}{\left(\hat{C} + \eta \tilde{C}(\chi) - e_C\right)}\left[\begin{matrix} -\mu_2/\left(\hat{R} + \eta \tilde{R}(\chi) - e_R\right) \\ +\mu_2/\left(\hat{R} + \eta \tilde{R}(\chi)\right) \end{matrix}\right] \\ &\quad - (\dot{r}_2 + \lambda_2 \chi_2)\left(1 + \frac{e_C}{\hat{C} + \eta \tilde{C}(\chi) - e_C}\right) \end{aligned} \tag{60}$$

From (59-60), we have:

$$\dot{\chi}_1 = -\lambda_1 \chi_1 - \frac{(\dot{r}_1 + \lambda_1 \chi_1) e_P}{\hat{L}_P + \eta \tilde{L}_P(\chi) - e_P} \tag{61}$$

$$\begin{aligned} \dot{\chi}_2 &= -\lambda_2 \chi_2 \\ &\quad \frac{-1}{\left(\hat{C} + \eta \tilde{C}(\chi) - e_C\right)}\left[\begin{matrix} -\mu_2/\left(\hat{R} + \eta \tilde{R}(\chi) - e_R\right) \\ +\mu_2/\left(\hat{R} + \eta \tilde{R}(\chi)\right) \\ +(\dot{r}_2 + \lambda_2 \chi_2) e_C \end{matrix}\right] \end{aligned} \tag{62}$$

Form (53-55), time derivative of e_P, e_R and e_C are computed as:

$$\dot{e}_P = \dot{\hat{L}}_P + \eta \frac{\partial \tilde{L}_P(\chi)}{\partial \chi_1} \dot{\chi}_1 + \eta \frac{\partial \tilde{L}_P(\chi)}{\partial \chi_2} \dot{\chi}_2 \tag{63}$$

$$\dot{e}_R = \dot{\hat{R}} + \eta \frac{\partial \tilde{R}(\chi)}{\partial \chi_1}\dot{\chi}_1 + \eta \frac{\partial \tilde{R}(\chi)}{\partial \chi_2}\dot{\chi}_2 \tag{64}$$

$$\dot{e}_C = \dot{\hat{C}} + \eta \frac{\partial \tilde{C}(\chi)}{\partial \chi_1}\dot{\chi}_1 + \eta \frac{\partial \tilde{C}(\chi)}{\partial \chi_2}\dot{\chi}_2 \tag{65}$$

Substituting $\dot{\chi}_1$ and $\dot{\chi}_2$, yields:

$$\begin{aligned}\dot{e}_P &= \dot{\hat{L}}_P + \eta \frac{\partial \tilde{L}_P(\chi)}{\partial \chi_1}\left[-\lambda_1\chi_1 - \frac{(\dot{r}_1 + \lambda_1\chi_1)\, e_P}{\hat{L}_P + \eta\tilde{L}_P(\chi) - e_P}\right] \\ &+ \eta \frac{\partial \tilde{L}_P(\chi)}{\partial \chi_2}\left[-\lambda_2\chi_2 - \frac{1}{\left(\hat{C}+\eta\tilde{C}(\chi)-e_C\right)}\left[\frac{-\mu_2 e_R}{\left(\hat{R}+\eta\tilde{R}(\chi)-e_R\right)\left(\hat{R}+\eta\tilde{R}(\chi)\right)} + (\dot{r}_2+\lambda_2\chi_2)\, e_C\right]\right]\end{aligned} \tag{66}$$

$$\begin{aligned}\dot{e}_R &= \dot{\hat{R}} + \eta \frac{\partial \tilde{R}(\chi)}{\partial \chi_1}\left[-\lambda_1\chi_1 - \frac{(\dot{r}_1 + \lambda_1\chi_1)\, e_P}{\hat{L}_P + \eta\tilde{L}_P(\chi) - e_P}\right] \\ &+ \eta \frac{\partial \tilde{R}(\chi)}{\partial \chi_2}\left[-\lambda_2\chi_2 - \frac{1}{\left(\hat{C}+\eta\tilde{C}(\chi)-e_C\right)}\left[\frac{-\mu_2 e_R}{\left(\hat{R}+\eta\tilde{R}(\chi)-e_R\right)\left(\hat{R}+\eta\tilde{R}(\chi)\right)} + (\dot{r}_2+\lambda_2\chi_2)\, e_C\right]\right]\end{aligned} \tag{67}$$

$$\begin{aligned}\dot{e}_C &= \dot{\hat{C}} + \eta \frac{\partial \tilde{C}(\chi)}{\partial \chi_1}\left[-\lambda_1\chi_1 - \frac{(\dot{r}_1 + \lambda_1\chi_1)\, e_P}{\hat{L}_P + \eta\tilde{L}_P(\chi) - e_P}\right] \\ &+ \eta \frac{\partial \tilde{C}(\chi)}{\partial \chi_2}\left[-\lambda_2\chi_2 - \frac{1}{\left(\hat{C}+\eta\tilde{C}(\chi)-e_C\right)}\left[\frac{-\mu_2 e_R}{\left(\hat{R}+\eta\tilde{R}(\chi)-e_R\right)\left(\hat{R}+\eta\tilde{R}(\chi)\right)} + (\dot{r}_2+\lambda_2\chi_2)\, e_C\right]\right]\end{aligned} \tag{68}$$

From (66-68), $\dot{\hat{L}}_P$, and $\dot{\hat{R}}$ and $\dot{\hat{C}}$ are considered as given in (31-33). From (31-33), $\dot{e}_P$, $\dot{e}_R$ and $\dot{e}_C$ in (66-68), become:

$$\begin{aligned}\dot{e}_P &= \eta \frac{\partial \tilde{L}_P(\chi)}{\partial \chi_1}\left[-\frac{(\dot{r}_1 + \lambda_1\chi_1)\, e_P}{\hat{L}_P + \eta\tilde{L}_P(\chi) - e_P}\right] + \eta \frac{\partial \tilde{L}_P(\chi)}{\partial \chi_2} \\ &\left[-\frac{1}{\left(\hat{C}+\eta\tilde{C}(\chi)-e_C\right)}\left[\frac{-\mu_2 e_R}{\left(\hat{R}+\eta\tilde{R}(\chi)-e_R\right)\left(\hat{R}+\eta\tilde{R}(\chi)\right)} + (\dot{r}_2+\lambda_2\chi_2)\, e_C\right]\right]\end{aligned} \tag{69}$$

$$\begin{aligned}\dot{e}_R &= \eta \frac{\partial \tilde{R}(\chi)}{\partial \chi_1}\left[-\frac{(\dot{r}_1 + \lambda_1\chi_1)\, e_P}{\hat{L}_P + \eta\tilde{L}_P(\chi) - e_P}\right] + \eta \frac{\partial \tilde{R}(\chi)}{\partial \chi_2} \\ &\left[-\frac{1}{\left(\hat{C}+\eta\tilde{C}(\chi)-e_C\right)}\left[\frac{-\mu_2 e_R}{\left(\hat{R}+\eta\tilde{R}(\chi)-e_R\right)\left(\hat{R}+\eta\tilde{R}(\chi)\right)} + (\dot{r}_2+\lambda_2\chi_2)\, e_C\right]\right]\end{aligned} \tag{70}$$

$$\begin{aligned}\dot{e}_C &= \eta \frac{\partial \tilde{C}(\chi)}{\partial \chi_1}\left[-\frac{(\dot{r}_1 + \lambda_1\chi_1)\, e_P}{\hat{L}_P + \eta\tilde{L}_P(\chi) - e_P}\right] + \eta \frac{\partial \tilde{C}(\chi)}{\partial \chi_2} \\ &\left[-\frac{1}{\left(\hat{C}+\eta\tilde{C}(\chi)-e_C\right)}\left[\frac{-\mu_2 e_R}{\left(\hat{R}+\eta\tilde{R}(\chi)-e_R\right)\left(\hat{R}+\eta\tilde{R}(\chi)\right)} + (\dot{r}_2+\lambda_2\chi_2)\, e_C\right]\right]\end{aligned} \tag{71}$$

From (69-71), $\tilde{L}_P(\chi)$, $\tilde{R}(\chi)$ and $\tilde{C}(\chi)$ should be determined such that the dynamics of $\dot{e}_P$, $\dot{e}_R$ and $\dot{e}_C$ to be stable. Then we have:

$$\frac{\partial \tilde{L}_P(\chi)}{\partial \chi_1} = \dot{r}_1 + \lambda_1\chi_1 \tag{72}$$

$$\frac{\partial \tilde{L}_P(\chi)}{\partial \chi_2} = 0 \tag{73}$$

$$\frac{\partial \tilde{R}(\chi)}{\partial \chi_1} = 0 \tag{74}$$

$$\frac{\partial \tilde{R}(\chi)}{\partial \chi_1} = -\left(\hat{R} + \eta\tilde{R}(\chi)\right) \tag{75}$$

$$\frac{\partial \tilde{C}(\chi)}{\partial \chi_1} = 0 \tag{76}$$

$$\frac{\partial \tilde{C}(\chi)}{\partial \chi_2} = \dot{r}_2 + \lambda_2\chi_2 \tag{77}$$

From (72-77), the dynamics of $\dot{e}_P$, $\dot{e}_R$ and $\dot{e}_C$ in (69-71), become:

$$\dot{e}_P = -\eta \frac{(\dot{r}_1 + \lambda_1\chi_1)^2}{\hat{L}_P + \eta\tilde{L}_P(\chi) - e_P} e_P \tag{78}$$

$$\begin{aligned}\dot{e}_R &= -\eta \frac{1}{\hat{C} + \eta\tilde{C}(\chi) - e_C} \cdot \frac{1}{\hat{R} + \eta\tilde{R}(\chi) - e_R}\mu_2 e_R \\ &+ \eta \frac{1}{\hat{C} + \eta\tilde{C}(\chi) - e_C}\left(\hat{R} + \eta\tilde{R}(\chi)\right)(\dot{r}_2 + \lambda_2\chi_2)\, e_C\end{aligned} \tag{79}$$

$$\begin{aligned}\dot{e}_C &= -\eta \frac{1}{\hat{C} + \eta\tilde{C}(\chi) - e_C} \cdot (\dot{r}_2 + \lambda_2\chi_2)^2 e_C \\ &+ \eta \frac{1}{\hat{C} + \eta\tilde{C}(\chi) - e_C} \cdot \frac{1}{\hat{R} + \eta\tilde{R}(\chi) - e_R} \\ &\cdot \frac{(\dot{r}_2 + \lambda_2\chi_2)\, \mu_2 e_R}{\hat{R} + \eta\tilde{R}(\chi)}\end{aligned} \tag{80}$$

To show that the dynamics of $\dot{e}_P$, $\dot{e}_R$ and $\dot{e}_C$ in (78-80) are stable, the following Lyapunov is considered:

$$V = \frac{1}{2}e_P^2 + \frac{1}{2}e_R^2 + \frac{1}{2}e_C^2 \tag{81}$$

Time derivative of (81), gives:

$$\dot{V} = e_P\dot{e}_P + e_R\dot{e}_R + e_C\dot{e}_C \tag{82}$$

substituting from (78-80), $\dot{V}$ in (82), becomes:

$$\begin{aligned}\dot{V} &= -\eta \frac{(\dot{r}_1 + \lambda_1\chi_1)^2}{\hat{L}_P + \eta\tilde{L}_P(\chi) - e_P} e_P^2 \\ &- \eta \frac{1}{\hat{C} + \eta\tilde{C}(\chi) - e_C} \cdot \frac{1}{\hat{R} + \eta\tilde{R}(\chi) - e_R}\mu_2 e_R^2 \\ &+ \eta \frac{1}{\hat{C} + \eta\tilde{C}(\chi) - e_C}\left(\hat{R} + \eta\tilde{R}(\chi)\right)(\dot{r}_2 + \lambda_2\chi_2)\, e_C e_R \\ &+ -\eta \frac{1}{\hat{C} + \eta\tilde{C}(\chi) - e_C} \cdot (\dot{r}_2 + \lambda_2\chi_2)^2 e_C^2 \\ &+ \eta \frac{1}{\hat{C} + \eta\tilde{C}(\chi) - e_C} \cdot \frac{1}{\hat{R} + \eta\tilde{R}(\chi) - e_R} \\ &\cdot \frac{(\dot{r}_2 + \lambda_2\chi_2)\, \mu_2 e_R e_C}{\hat{R} + \eta\tilde{R}(\chi)}\end{aligned} \tag{83}$$

$\dot{V}$ is rewritten as:

$$\dot{V} = -\begin{bmatrix} e_P & e_R & e_C \end{bmatrix} \Psi \begin{bmatrix} e_P \\ e_R \\ e_C \end{bmatrix} \tag{84}$$

where,

$$\Psi_{11} = \eta \frac{(\dot{r}_1 + \lambda_1 \chi_1)^2}{\hat{L}_P + \eta \tilde{L}_P(\chi) - e_P} \tag{85}$$

$$\Psi_{12} = \frac{1}{\hat{C}+\eta\tilde{C}(\chi) - e_C} \frac{1}{\hat{R} + \eta\tilde{R}(\chi) - e_R} \cdot \frac{(\dot{r}_2 + \lambda_2\chi_2)\mu_2}{\hat{R} + \eta\tilde{R}(\chi)} + \frac{1}{\hat{C} + \eta\tilde{C}(\chi) - e_C}\left(\hat{R} + \eta\tilde{R}(\chi)\right)(\dot{r}_2 + \lambda_2\chi_2) \tag{86}$$

$$\Psi_{22} = \eta \frac{1}{\hat{C} + \eta\tilde{C}(\chi) - e_C} \cdot (\dot{r}_2 + \lambda_2\chi_2)^2 \tag{87}$$

From the fact that:

$$C = \hat{C} + \eta\tilde{C}(\chi) - e_C > 0 \tag{88}$$

$$R = \hat{R} + \eta\tilde{R}(\chi) - e_R > 0 \tag{89}$$

$$L_P = \hat{L}_P + \eta\tilde{L}_P(\chi) - e_P > 0 \tag{90}$$

It is concluded that by properly choosing λ_1 and λ_2, Ψ is positive definite and then the dynamics of $\dot{e}_P$, $\dot{e}_R$ and $\dot{e}_C$ are stable. □

V. DEEP LEARNED TYPE-2 FUZZY COMPENSATOR

To ensure the stability in versus of I&I approximation error an AT2FLC is presented. The outcomes are given in Theorem 2.

Theorem 2: The stability of the tracking error dynamics (61-62) is ensued in versus of I&I approximation error and dynamic perturbation by the following modified controllers and tuning rules of AT2FLCs:

$$u_p = \frac{1}{\mu_2}\begin{bmatrix} (\dot{r}_1 + \lambda_1\chi_1)\left(\hat{L}_P + \eta\tilde{L}_P(\chi)\right) \\ +\mu_2 - V_p(\mu_1) + u_{cp}\left(z_p|X_p\right) \end{bmatrix} \tag{91}$$

$$u_b = \frac{1}{\mu_3}\begin{bmatrix} (\dot{r}_2 + \lambda_2\chi_2)\left(\hat{C} + \eta\tilde{C}(\chi)\right) - \mu_1 + \\ \mu_2/\left(\hat{R} + \eta\tilde{R}(\chi)\right) + \mu_1 u_p + u_{cb}(z_b|X_b) \end{bmatrix} \tag{92}$$

$$\dot{z}_p = \gamma\pi_p\chi_1 \tag{93}$$

$$\dot{z}_b = \gamma\pi_b\chi_2 \tag{94}$$

where, $u_{cp}\left(z_p|X_p\right)$ and $u_{cb}(z_b|X_b)$ are AT2FLCs. γ is a constant.

Proof: To deeply train the fuzzy compensator by Lyapunov approach, the outputs $u_{cp}\left(z_p|X_p\right)$ and $u_{cb}(z_b|X_b)$ (see (23)) are written as:

$$u_{cp}\left(z_p|X_p\right) = z_p^T\pi_p$$
$$u_{cb}(z_b|X_b) = z_b^T\pi_b \tag{95}$$

where, z_p^T and z_b^T are vector of tuneable parameters which include both rule (consequent) parameters (z_{pc}^T, z_{bc}^T) and centers of FSs (antecedent parameters: z_{pa}^T, z_{ba}^T):

$$z_p^T = \left[z_{pa}^T\, z_{pc}^T\right]$$
$$z_b^T = \left[z_{ba}^T\, z_{bc}^T\right] \tag{96}$$

π_p^T and π_b^T are written as:

$$\pi_p^T = \left[\pi_{pa}^T\, \pi_{pc}^T\right]$$
$$\pi_b^T = \left[\pi_{ba}^T\, \pi_{bc}^T\right] \tag{97}$$

where,

$$\pi_{pc}^T = \frac{1}{\sum_{i=1}^{N}\bar{\theta}_{pi} + \underline{\theta}_{pi}}\left[\bar{\theta}_{p1} + \underline{\theta}_{p1}, \ldots, \bar{\theta}_{pN} + \underline{\theta}_{pN}\right]^T$$

$$\pi_{bc}^T = \frac{1}{\sum_{i=1}^{N}\bar{\theta}_{bi} + \underline{\theta}_{bi}}\left[\bar{\theta}_{b1} + \underline{\theta}_{b1}, \ldots, \bar{\theta}_{bN} + \underline{\theta}_{bN}\right]^T \tag{98}$$

where, $\bar{\theta}_{pi}$ and $\bar{\theta}_{bi}$ are upper rule firing and $\underline{\theta}_{pi}$ and $\underline{\theta}_{bi}$ are lower rule firings. The other terms π_{pa}^T and π_{ba}^T are derivative of $u_{cp}\left(z_p|X_p\right)$ and $u_{cb}(z_b|X_b)$ with respect to the centers of FSs. For instance, the derivatives for $M_{\bar{\vartheta}_\chi}$ can be obtained as:

$$\frac{\partial u_{cp}\left(z_p|X_p\right)}{\partial M_{\bar{\vartheta}_\chi}} = \begin{bmatrix} \frac{2\left(\chi(t) - M_{\bar{\vartheta}_\chi}\right)}{\bar{\sigma}_{\bar{\vartheta}_\chi}^2}\sum_{i=1}^{N/2}\bar{\theta}_{pi} \\ +\frac{2\left(\chi(t) - M_{\bar{\vartheta}_\chi}\right)}{\underline{\sigma}_{\bar{\vartheta}_\chi}^2}\sum_{i=1}^{N/2}\underline{\theta}_{pi} \end{bmatrix} z_{pi}\Big/\sum_{i=1}^{N}\bar{\theta}_{bi} + \underline{\theta}_{bi} - \sum_{i=1}^{N} z_{pi}\left(\bar{\theta}_{pi} + \underline{\theta}_{pi}\right) \cdot \begin{bmatrix} \frac{2\left(\chi(t) - M_{\bar{\vartheta}_\chi}\right)}{\bar{\sigma}_{\bar{\vartheta}_\chi}^2}\sum_{i=1}^{N/2}\bar{\theta}_{pi} \\ +\frac{2\left(\chi(t) - M_{\bar{\vartheta}_\chi}\right)}{\underline{\sigma}_{\bar{\vartheta}_\chi}^2}\sum_{i=1}^{N/2}\underline{\theta}_{pi} \end{bmatrix} \Big/ \left(\sum_{i=1}^{N}\bar{\theta}_{bi} + \underline{\theta}_{bi}\right)^2 \tag{99}$$

By applying controllers (91-92), the error dynamics become:

$$\dot{\chi}_1 = -\lambda_1\chi_1 - \frac{\left(\dot{r}_1 + \lambda_1\chi_1 + u_{cp}\left(z_p|X_p\right)\right)e_P}{\hat{L}_P + \eta\tilde{L}_P(\chi) - e_P} \tag{100}$$

$$\dot{\chi}_2 = -\lambda_2\chi_2 - \frac{1}{\left(\hat{C} + \eta\tilde{C}(\chi) - e_C\right)} \times \left[\frac{-\mu_2 e_R}{\left(\hat{R} + \eta\tilde{R}(\chi) - e_R\right)\left(\hat{R} + \eta\tilde{R}(\chi)\right)} + \left(\dot{r}_2 + \lambda_2\chi_2 + u_{cb}(z_b|X_b)\right)e_C\right] \tag{101}$$

By adding and subtracting optimal AT2FLCs $u_{cp}\left(z_p^*|X_p\right)$ and $u_{cb}\left(z_b^*|X_b\right)$, the dynamics (100-101) are rewritten as:

$$\dot{\chi}_1 = -\lambda_1\chi_1 + u_{cp}\left(z_p^*|X_p\right) - u_{cp}\left(z_p|X_p\right) - \frac{\left(\dot{r}_1 + \lambda_1\chi_1 + u_{cp}\left(z_p|X_p\right)\right)e_P}{\hat{L}_P + \eta\tilde{L}_P(\chi) - e_P} - u_{cp}\left(z_p^*|X_p\right) \tag{102}$$

$$\dot{\chi}_2 = -\lambda_2\chi_2 + u_{cb}\left(z_b^*|X_b\right) - u_{cb}(z_b|X_b) - \frac{1}{\left(\hat{C} + \eta\tilde{C}(\chi) - e_C\right)}$$

$$\times\left[\frac{-\mu_2 e_R}{\left(\hat{R}+\eta\tilde{R}(\chi)-e_R\right)\left(\hat{R}+\eta\tilde{R}(\chi)\right)} + \left(\dot{r}_2+\lambda_2\chi_2+u_{cb}(z_b|X_b)\right)e_C\right] - u_{cb}\left(z_b^*|X_b\right) \quad (103)$$

From (23), we have:

$$u_{cb}\left(z_b^*|X_b\right) - u_{cb}\left(z_b|X_b\right) = \tilde{z}_b\pi_b \quad (104)$$
$$u_{cp}\left(z_p^*|X_p\right) - u_{cp}\left(z_p|X_p\right) = \tilde{z}_p\pi_p \quad (105)$$

where,

$$\tilde{z}_b = z_b^* - z_b \quad (106)$$
$$\tilde{z}_p = z_p^* - z_p \quad (107)$$

From (104-105), the equations (102-103), are written as:

$$\dot{\chi}_1 = -\lambda_1\chi_1 + \tilde{z}_p\pi_p - \frac{\left(\dot{r}_1+\lambda_1\chi_1+u_{cp}\left(z_p|X_p\right)\right)e_P}{\hat{L}_P+\eta\tilde{L}_P(\chi)-e_P} - u_{cp}\left(z_p^*|X_p\right) \quad (108)$$

$$\dot{\chi}_2 = -\lambda_2\chi_2 + \tilde{z}_b\pi_b - \frac{1}{\left(\hat{C}+\eta\tilde{C}(\chi)-e_C\right)} \times\left[\frac{-\mu_2 e_R}{\left(\hat{R}+\eta\tilde{R}(\chi)-e_R\right)\left(\hat{R}+\eta\tilde{R}(\chi)\right)} + \left(\dot{r}_2+\lambda_2\chi_2+u_{cb}(z_b|X_b)\right)e_C\right] - u_{cb}\left(z_b^*|X_b\right) \quad (109)$$

Consider the following definitions:

$$\varepsilon_p^* = -\frac{\left(\dot{r}_1+\lambda_1\chi_1+u_{cp}\left(z_p|X_p\right)\right)e_P}{\hat{L}_P+\eta\tilde{L}_P(\chi)-e_P} - u_{cp}\left(z_p^*|X_p\right) \quad (110)$$

$$\varepsilon_b^* = \frac{1}{\left(\hat{C}+\eta\tilde{C}(\chi)-e_C\right)}\left[\frac{-\mu_2 e_R}{\left(\hat{R}+\eta\tilde{R}(\chi)-e_R\right)\left(\hat{R}+\eta\tilde{R}(\chi)\right)} + \left(\dot{r}_2+\lambda_2\chi_2+u_{cb}(z_b|X_b)\right)e_C\right] - u_{cb}\left(z_b^*|X_b\right) \quad (111)$$

Considering definitions (110-111), equations (108-109), become:

$$\dot{\chi}_1 = -\lambda_1\chi_1 + \tilde{z}_p\pi_p + \varepsilon_p^* \quad (112)$$
$$\dot{\chi}_2 = -\lambda_2\chi_2 + \tilde{z}_b\pi_b + \varepsilon_b^* \quad (113)$$

To investigate the stability, the following Lyapunov is taken to account:

$$V = \frac{1}{2}\chi_1^2 + \frac{1}{2}\chi_2^2 + \frac{1}{2\gamma}\tilde{z}_p^2 + \frac{1}{2\gamma}\tilde{z}_b^2 \quad (114)$$

From (114), $\dot{V}$ is obtained as:

$$\dot{V} = \chi_1\dot{\chi}_1 + \chi_2\dot{\chi}_2 - \frac{1}{\gamma}\tilde{z}_p\dot{z}_p - \frac{1}{\gamma}\tilde{z}_b\dot{z}_b \quad (115)$$

By substituting (112-113), $\dot{V}$ becomes:

$$\dot{V} = \chi_1\left(-\lambda_1\chi_1 + \tilde{z}_p\pi_p + \varepsilon_p^*\right) + \chi_2\left(-\lambda_2\chi_2 + \tilde{z}_b\pi_b + \varepsilon_b^*\right) - \frac{1}{\gamma}\tilde{z}_p\dot{z}_p - \frac{1}{\gamma}\tilde{z}_b\dot{z}_b \quad (116)$$

TABLE 1. Simulation condition.

Parameter	value	Parameter	value
L_p	6 (mH)	L_b	15 (mH)
Q	1.60e-19	n	36
P_{PV}	55 (w)	i_{sc}	3.55 (A)
C	500 (μf)	r_p	30 $(m\Omega)$
r_b	80 $(m\Omega)$	k_b	1.38e-23
T_r	$(°C)$	k_i	1.5 (A/k)
A	1.2	V_{boc}	15 (v)
i_r	5.980e-8 (A)	E_g	1.120 (ev)
β_1	0.85	β_2	1.15
P_b	20 (w)	E_{Loss}	25 (w)

Equation (116), can be written as:

$$\dot{V} = -\lambda_1\chi_1^2 - \lambda_2\chi_2^2 + \tilde{z}_p\pi_p\chi_1 + \tilde{z}_b\pi_b\chi_2 + \chi_1\varepsilon_p^* + \chi_2\varepsilon_b^* - \frac{1}{\gamma}\tilde{z}_p\dot{z}_p - \frac{1}{\gamma}\tilde{z}_b\dot{z}_b \quad (117)$$

The equation (117) is simplified as:

$$\dot{V} = -\lambda_1\chi_1^2 - \lambda_2\chi_2^2 + \tilde{z}_p\left(\pi_p\chi_1 - \frac{1}{\gamma}\dot{z}_p\right) + \tilde{z}_b\left(\pi_b\chi_2 - \frac{1}{\gamma}\dot{z}_b\right) + \chi_1\varepsilon_p^* + \chi_2\varepsilon_b^* \quad (118)$$

From tuning rules of AT2FLCs (93-94), $\dot{V}$ is written as:

$$\dot{V} = -\lambda_1\chi_1^2 - \lambda_2\chi_2^2 + \chi_1\varepsilon_p^* + \chi_2\varepsilon_b^* \quad (119)$$

From (119), we have:

$$\dot{V} \le -\lambda_1\chi_1^2 - \lambda_2\chi_2^2 + \chi_1^2\bar{\varepsilon}_p^* + \chi_2^2\bar{\varepsilon}_b^* \quad (120)$$

The $\bar{\varepsilon}_p^*$ and $\bar{\varepsilon}_b^*$ are the upper bounds of ε_p^* and ε_b^*. Then if:

$$\lambda_1 > \bar{\varepsilon}_p^*$$
$$\lambda_2 > \bar{\varepsilon}_b^* \quad (121)$$

The asymptotically stability is ensured. □

VI. SIMULATION STUDIES

Several examinations are presented in this section. Simulation condition is described in Table 1.

A. SCENARIO 1

For first evaluation, the irradiation is considered to be varied from 250 to 650 (w/m^2) at time $t = 50$s. Fig. 7, shows that the PV current is well converged to its target level. Fig. 8 demonstrates that the voltage V_c is kept fixed at its desired level under irradiation disturbances. Fig. 9 shows the well power regulation and finally Figs. 10-11 show the control signals with good shapes and lack of fluctuations.

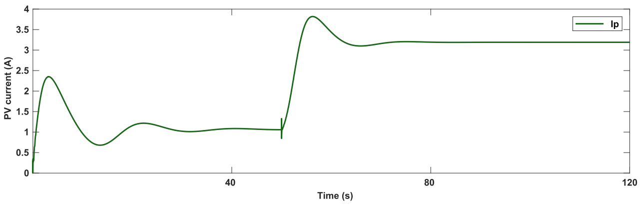

FIGURE 7. Scenario 1: PV current (I_P).

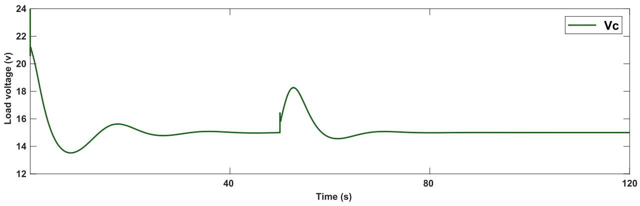

FIGURE 8. Scenario 1: Output voltage (V_C).

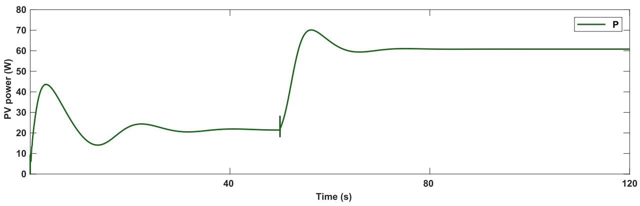

FIGURE 9. Scenario 1: PV power (P).

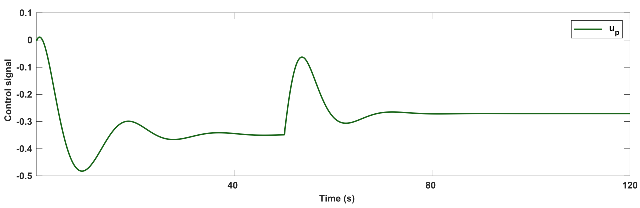

FIGURE 10. Scenario 1: Control signal (u_p).

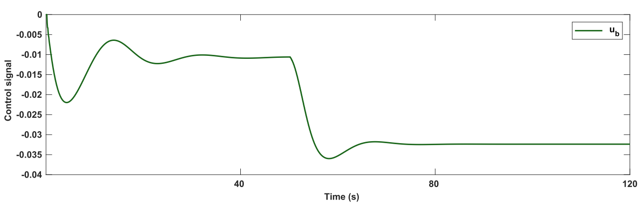

FIGURE 11. Scenario 1: Control signal (u_b).

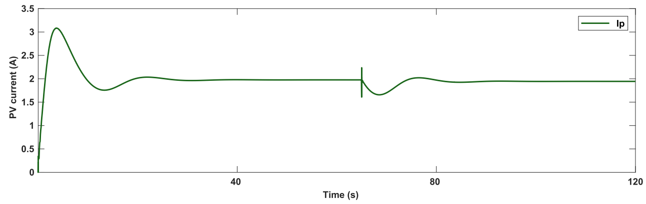

FIGURE 12. Scenario 2: PV current (I_P).

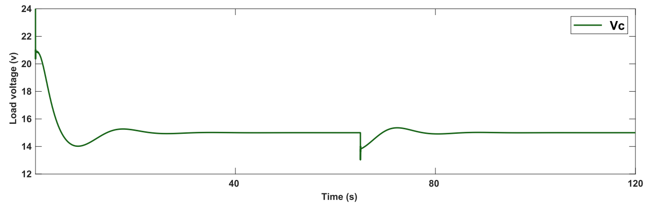

FIGURE 13. Scenario 2: Output voltage (V_C).

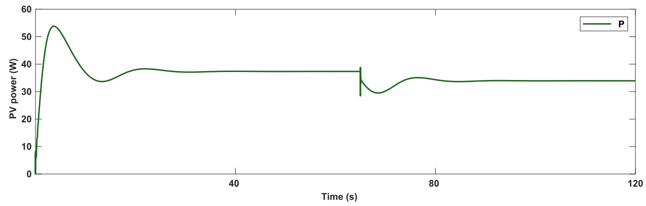

FIGURE 14. Scenario 2: PV power (P).

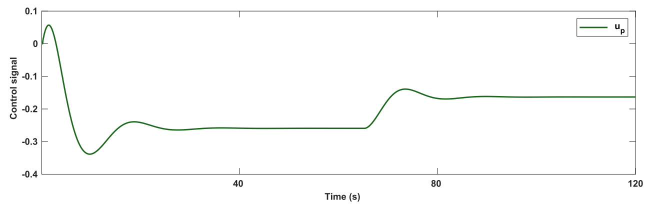

FIGURE 15. Scenario 2: Control signal (u_p).

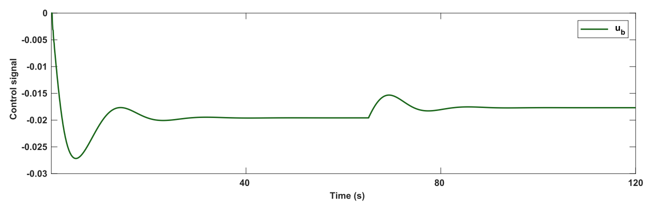

FIGURE 16. Scenario 2: Control signal (u_b).

B. SCENARIO 2

For second evaluation, the irradiation is fixed at 400 (w/m^2) and the temperature disturbances is changed from $T = 15$ into $T = 38$ $(°C)$ at time $t = 65$s. Fig. 12 shows that the PV current well tracks the reference trajectory. Fig. 13 shows a well resistance in versus of temperature variation. Fig. 14 shows the power regulation, and Figs. 15-16 show the control trajectories.

C. SCENARIO 3

For scenario 3, in the difficult examination situation, the temperature, load and irradiation are changed from $T = 13$ to $T = 48$ $(°C)$, 60 into 40 (Ω) from 450 into 150 (w/m^2), respectively. The disturbances are depicted in Fig. 17. Fig. 18 shows that PV current tracks its optimal trajectory in versus of different perturbations. Fig. 19 reveals that the output vorlage strongly tackles the effect of disturbances. Fig. 20 shows a desired power regulation, and finally Figs. 21-22 show the control signal with implementable shapes.

D. COMPARISON

In this section, a comparison is presented with Fractional-order-PID (FO-PID) [38], integral sliding mode controller (SMC) [39], fuzzy PID [40] and intelligent controller by Levy

TABLE 2. RMSE comparison.

Signal	Method				
	FO-PID [38]	Integral SMC [39]	Fuzzy PID [40]	ILWO [41]	I&I
V_c	3.0168	1.7208	2.3067	1.8612	1.5006

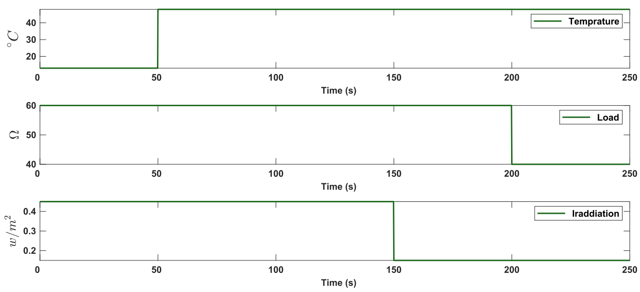

FIGURE 17. Scenario 3: Variation of temperature, load and irradiation.

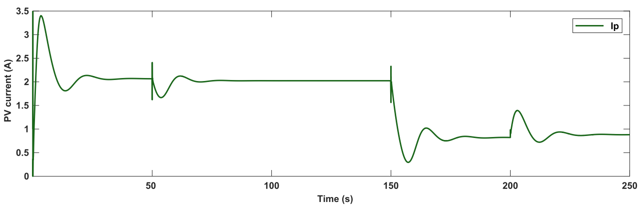

FIGURE 18. Scenario 3: PV current (I_P).

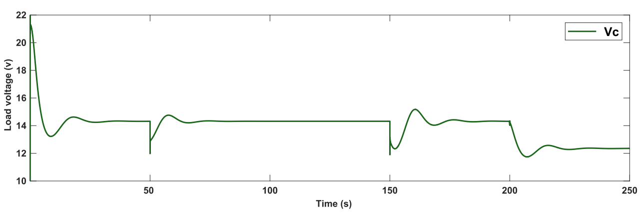

FIGURE 19. Scenario 3: Output voltage (V_C).

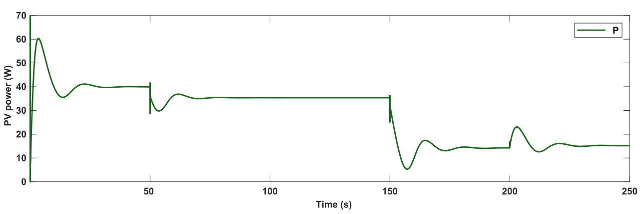

FIGURE 20. Scenario 3: PV power (P).

Whale Optimization (ILWO) [41]. The values of root-mean-square-errors (RMSEs) are depicted in Table 2. We see that, the presented I&I method outperforms than other conventional approaches.

Remark 1: The main properties of the designed control technique are that: (1) there is no strong dependency on the mathematical models of units, (2) the new adaptation rules which are extracted form I&I stability theorem, well ensure the stability, (3) the designed T2FLC well compensate the approximation error and perturbations, (4) the designed controller shows a good robust efficiency. To examine the

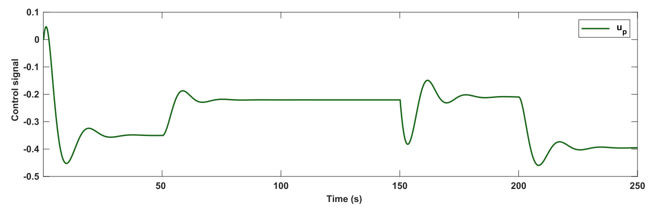

FIGURE 21. Scenario 3: Control signal (u_p).

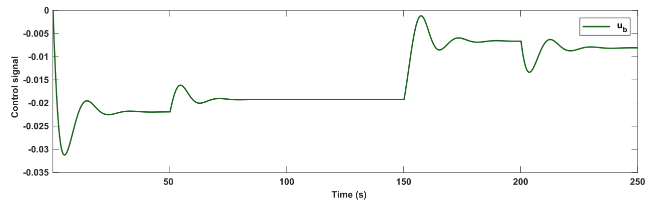

FIGURE 22. Scenario 3: Control signal (u_b).

robustness, in various scenarios, the irradiation is considered to be varied from 250 to 650 (w/m^2), the temperature disturbances is changed from $T = 15$ into $T = 38$ ($°C$), the output load is changed from 60 into 40 (Ω), and output power/voltage regulation is evaluated. Simulations show that a good regulation is achieved under aforementioned disturbances and unknown dynamics. Furthermore, a comparison with other conventional approaches such as FO-PID [38], Integral SMC [39], Fuzzy PID [40], and ILWO [41], better reveals the superiority of the suggested I&I-based controller.

Remark 2: It should be noted that, in the most of previous conventional learning approaches, it is needed that the learning algorithms to be repeated in some epochs. However, in the suggested approach, T2FLCs are online updated based on the learning laws that are extracted from I&I theorem, and there is no need to any iterations. In other words, at each sample time, both rules and FS parameters are updated at once. At each sample time, the parameters of rules and FSs are obtained by taking the integral form adaptation rules (93- 94). Then, there is no huge computations and its implementation is quite feasible.

VII. CONCLUSION

In this paper a new strategy is developed based on I&I approach for voltage regulation in PV/FC/Battery systems. Some tuning rules are presented for uncertain parameters such that the I&I stabilization criterions are satisfied. The perturbations are compensated by the a suggested deep learning T2FLC. In three faulty conditions the performance is evaluated. For first one, irradiation is suddenly changed from its nominal level, it is shown the PV power well tracks its optimal target, and the output voltage is also well regulated on its reference set point. For the second examination, the effect of variation of temperature is taken to account, and temperature is considered to be time-varying. The simulations show a good resistance against temperature disturbance. Finally, for the last examination, beside variation of temperature and irradiation, the output load is also considered to be time-varying. Simulation results and comparison with other new controllers demonstrates that the suggested control scenario results in better regulation proficiency under uncertain dynamics and difficult faulty conditions.

APPENDIX
PARAMETERS DESCRIPTIONS

TABLE 3. Parameter definition, see equation (1).

Parameter	Definition	Unit
$\Re$	Gas constant	J/mol K
ξ_{H_2O}	Water partial pressures	atm
T	Stack temperature	kelvin
E_0	Voltage for reaction free energy	(volts)
ι	Internal resistance	ohms
I_{IC}	Current	A
ξ_{H_2}	Hydrogen partial pressure	atm
N_0	Number of cells	-
ξ_{O_2}	Oxygen partial pressure	atm
F	Faraday's constant	C/mol

TABLE 4. Parameter definition, see equations (2-6).

Parameter	Definition	Unit
k_{H_2}	Index of Hydrogen valve molar	kmol/s· atm
κ_{H_2}	Hydrogen time constant	sec
k_{H_2O}	Index of Water valve molar	kmol/s· atm
κ_{O_2}	Oxygen time constant	sec
k_{O_2}	Index of Oxygen valve molar	kmol/s · atm
κ_{H_2O}	Water time constant	sec
ι_{HO}	Ratio of hydrogen to oxygen	-
Q_{H_2}	Hydrogen flow rate	mol/s
τ_ι	Constant	kmol/s · A
Q_{O_2}	Oxygen flow rate	mol/s
U_{opt}	Optimal fuel employment	-
κ_f	Fuel time constant	sec

TABLE 5. PV parameter definition, see equation (8).

Parameter	Description
n	Number of cells
$G\,(w/m^2)$	Solar radiation
Q	Electron charge
$E_g\,(ev)$	Energy of Band-Gap
$T\,(^\circ c)$	Temperature of PV
$k_b\,(J/\tau)$	Boltzmann's constant
$\Re_{sh}$ and $\Re_s\,(\Omega)$	Equivalent resistances
A	Diode ideality constant
$i_\iota\,(A)$	Saturation current
$T_\iota\,(^\circ c)$	Target temperature
$i_{ph}\,(A)$	Photo generated currents

TABLE 6. Battery parameters definition, see equation (11).

Parameter	Definition
$\iota_b\,(\Omega)$	Internal resistance
$V_{boc}\,(v)$	Open circuit voltage
$E_{Loss}\,(w)$	Power losses
$E_{\mathrm{Max}}\,(J)$	Maximum chargeable energy
β_1 and β_2	Charge/Discharge rates

REFERENCES

[1] H. Gholami-Khesht, P. Davari, and F. Blaabjerg, "An adaptive model predictive voltage control for LC-filtered voltage source inverters," *Appl. Sci.*, vol. 11, no. 2, p. 704, Jan. 2021, doi: 10.3390/app11020704.

[2] H. J. Queen, J. Jayakumar, T. Deepika, K. V. S. M. Babu, and S. P. Thota, "Machine learning-based predictive techno-economic analysis of power system," *IEEE Access*, vol. 9, pp. 123504–123516, 2021.

[3] Y. Zhao, F. Cheng, S. Yuksel, and H. Dincer, "Integer code series enhanced IT2 fuzzy decision support system with alpha cuts for the innovation adoption life cycle pattern recognition of renewable energy alternatives," *IEEE Access*, vol. 9, pp. 34906–34920, 2021.

[4] F. Cheng, M. Lin, S. Yuksel, H. Dincer, and H. Kalkavan, "A hybrid hesitant 2-tuple IVSF decision making approach to analyze PERT-based critical paths of new service development process for renewable energy investment projects," *IEEE Access*, vol. 9, pp. 3947–3969, 2021.

[5] U. Subramaniam, S. Vavilapalli, S. Padmanaban, F. Blaabjerg, J. B. Holm-Nielsen, and D. Almakhles, "A hybrid PV-battery system for ON-grid and OFF-grid applications—Controller-in-loop simulation validation," *Energies*, vol. 13, no. 3, p. 755, Feb. 2020, doi: 10.3390/en13030755.

[6] C. Lupangu, J. J. Justo, and R. C. Bansal, "Model predictive for reactive power scheduling control strategy for PV–battery hybrid system in competitive energy market," *IEEE Syst. J.*, vol. 14, no. 3, pp. 4071–4078, Sep. 2020, doi: 10.1109/JSYST.2020.2968926.

[7] M. Elkazaz, M. Sumner, and D. Thomas, "Energy management system for hybrid PV-wind-battery microgrid using convex programming, model predictive and rolling horizon predictive control with experimental validation," *Int. J. Electr. Power Energy Syst.*, vol. 115, Feb. 2020, Art. no. 105483, doi: 10.1016/j.ijepes.2019.105483.

[8] S.-I. Go and J.-H. Choi, "Design and dynamic modelling of PV-battery hybrid systems for custom electromagnetic transient simulation," *Electronics*, vol. 9, no. 10, p. 1651, Oct. 2020, doi: 10.3390/electronics9101651.

[9] V. P. Chandran, S. Kewat, and B. Singh, "Multi-objective control and operation of grid-connected small hydro-solar PV-battery energy storage-based distributed generation," *IET Renew. Power Gener.*, vol. 14, no. 16, pp. 3259–3272, Dec. 2020, doi: 10.1049/iet-rpg.2020.0212.

[10] Y. Han, H. Yang, Q. Li, W. Chen, F. Zare, and J. M. Guerrero, "Mode-triggered droop method for the decentralized energy management of an islanded hybrid PV/hydrogen/battery DC microgrid," *Energy*, vol. 199, May 2020, Art. no. 117441, doi: 10.1016/j.energy.2020.117441.

[11] Y. Singh, B. Singh, and S. Mishra, "Multifunctional control for PV-integrated battery energy storage system with improved power quality," *IEEE Trans. Ind. Appl.*, vol. 56, no. 6, pp. 6835–6845, Nov. 2020, doi: 10.1109/TIA.2020.3020528.

[12] J. Lai and X. Lu, "Robust self-consistent control of PV-battery-based microgrids without continuous communication," *Int. J. Electr. Power Energy Syst.*, vol. 119, Jul. 2020, Art. no. 105900, doi: 10.1016/j.ijepes.2020.105900.

[13] A. Y. Ali, A. Basit, T. Ahmad, A. Qamar, and J. Iqbal, "Optimizing coordinated control of distributed energy storage system in microgrid to improve battery life," *Comput. Electr. Eng.*, vol. 86, Sep. 2020, Art. no. 106741, doi: 10.1016/j.compeleceng.2020.106741.

[14] A. M. Bozorgi, H. Gholami-Khesht, M. Farasat, S. Mehraeen, and M. Monfared, "Model predictive direct power control of three-phase grid-connected converters with fuzzy-based duty cycle modulation," *IEEE Trans. Ind. Appl.*, vol. 54, no. 5, pp. 4875–4885, Sep./Oct. 2018, doi: 10.1109/TIA.2018.2839660.

[15] T. Mahto, H. Malik, V. Mukherjee, M. A. Alotaibi, and A. Almutairi, "Renewable generation based hybrid power system control using fractional order-fuzzy controller," *Energy Rep.*, vol. 7, pp. 641–653, Nov. 2021.

[16] M. Abbas and D. Zhang, "A smart fault detection approach for PV modules using adaptive neuro-fuzzy inference framework," *Energy Rep.*, vol. 7, pp. 2962–2975, Nov. 2021.

[17] I. Abadlia, L. Hassaine, A. Beddar, F. Abdoune, and M. R. Bengourina, "Adaptive fuzzy control with an optimization by using genetic algorithms for grid connected a hybrid photovoltaic–hydrogen generation system," *Int. J. Hydrogen Energy*, vol. 45, no. 43, pp. 22589–22599, Sep. 2020, doi: 10.1016/j.ijhydene.2020.06.168.

[18] A. Shaban, H. Maher, M. Elbayoumi, and S. Abdelhady, "A cuckoo load scheduling optimization approach for smart energy management," *Energy Rep.*, vol. 7, pp. 4705–4721, Nov. 2021.

[19] A. Al-Hinai, H. Alyammahi, and H. H. Alhelou, "Coordinated intelligent frequency control incorporating battery energy storage system, minimum variable contribution of demand response, and variable load damping coefficient in isolated power systems," *Energy Rep.*, vol. 7, pp. 8030–8041, Nov. 2021.

[20] A. A. Kamel, H. Rezk, and M. A. Abdelkareem, "Enhancing the operation of fuel cell-photovoltaic-battery-supercapacitor renewable system through a hybrid energy management strategy," *Int. J. Hydrogen Energy*, vol. 46, no. 8, pp. 6061–6075, Jan. 2021, doi: 10.1016/j.ijhydene.2020.06.052.

[21] Z. Mokrani, D. Rekioua, and T. Rekioua, "Modeling, control and power management of hybrid photovoltaic fuel cells with battery bank supplying electric vehicle," *Int. J. Hydrogen Energy*, vol. 39, no. 27, pp. 15178–15187, Sep. 2014, doi: 10.1016/j.ijhydene.2014.03.215.

[22] C. Conker and M. K. Baltacioglu, "Fuzzy self-adaptive PID control technique for driving HHO dry cell systems," *Int. J. Hydrogen Energy*, vol. 45, no. 49, pp. 26059–26069, Oct. 2020, doi: 10.1016/j.ijhydene.2020.01.136.

[23] H. Rezk, A. M. Nassef, M. A. Abdelkareem, A. H. Alami, and A. Fathy, "Comparison among various energy management strategies for reducing hydrogen consumption in a hybrid fuel cell/supercapacitor/battery system," *Int. J. Hydrogen Energy*, vol. 46, no. 8, pp. 6110–6126, Jan. 2021, doi: 10.1016/j.ijhydene.2019.11.195.

[24] S. Sennan, S. Ramasubbareddy, S. Balasubramaniyam, A. Nayyar, M. Abouhawwash, and N. A. Hikal, "T2FL-PSO: Type-2 fuzzy logic-based particle swarm optimization algorithm used to maximize the lifetime of Internet of Things," *IEEE Access*, vol. 9, pp. 63966–63979, 2021.

[25] V. K. Menaria, S. C. Jain, N. Raju, R. Kumari, A. Nayyar, and E. Hosain, "NLFFT: A novel fault tolerance model using artificial intelligence to improve performance in wireless sensor networks," *IEEE Access*, vol. 8, pp. 149231–149254, 2020.

[26] A. Al-Mahturi, F. Santoso, M. A. Garratt, and S. G. Anavatti, "Self-learning in aerial robotics using type-2 fuzzy systems: Case study in hovering quadrotor flight control," *IEEE Access*, vol. 9, pp. 119520–119532, 2021.

[27] A. Al-Mahturi, F. Santoso, M. A. Garratt, and S. G. Anavatti, "Online system identification for nonlinear uncertain dynamical systems using recursive interval type-2 TS fuzzy C-means clustering," in *Proc. IEEE Symp. Ser. Comput. Intell. (SSCI)*, Dec. 2020, pp. 1695–1701.

[28] S. B. Pandu, C. K. Sundarabalan, N. S. Srinath, T. S. Krishnan, G. S. Priya, C. Balasundar, J. Sharma, G. Soundarya, P. Siano, and H. H. Alhelou, "Power quality enhancement in sensitive local distribution grid using interval type-II fuzzy logic controlled DSTATCOM," *IEEE Access*, vol. 9, pp. 59888–59899, 2021.

[29] B. Chelladurai, C. K. Sundarabalan, S. N. Santhanam, and J. M. Guerrero, "Interval type-2 fuzzy logic controlled shunt converter coupled novel high-quality charging scheme for electric vehicles," *IEEE Trans. Ind. Informat.*, vol. 17, no. 9, pp. 6084–6093, Sep. 2021.

[30] C.-L. Zhang, X.-Z. Wu, and J. Xu, "Particle swarm sliding mode-fuzzy PID control based on maglev system," *IEEE Access*, vol. 9, pp. 96337–96344, 2021.

[31] Z. Liu, A. Mohammadzadeh, H. Turabieh, M. Mafarja, S. S. Band, and A. Mosavi, "A new online learned interval type-3 fuzzy control system for solar energy management systems," *IEEE Access*, vol. 9, pp. 10498–10508, 2021, doi: 10.1109/ACCESS.2021.3049301.

[32] A. Mohammadzadeh and S. Rathinasamy, "Energy management in photovoltaic battery hybrid systems: A novel type-2 fuzzy control," *Int. J. Hydrogen Energy*, vol. 45, no. 41, pp. 20970–20982, Aug. 2020, doi: 10.1016/j.ijhydene.2020.05.187.

[33] L. Sheng and X. Ma, "Stability analysis and controller design of interval type-2 fuzzy systems with time delay," *Int. J. Syst. Sci.*, vol. 45, no. 5, pp. 977–993, May 2014.

[34] A. Mohammadzadeh and F. Hashemzadeh, "A new robust observer-based adaptive type-2 fuzzy control for a class of nonlinear systems," *Appl. Soft Comput.*, vol. 37, pp. 204–216, Dec. 2015.

[35] L. Sheng and X. Ma, "Stability analysis and controller design of discrete interval type-2 fuzzy systems," *Asian J. Control*, vol. 16, no. 4, pp. 1091–1104, Jul. 2014.

[36] B. Lin, "Conceptual design and modeling of a fuel cell scooter for urban Asia," *J. Power Sources*, vol. 86, nos. 1–2, pp. 202–213, 2000, doi: 10.1016/S0378-7753(99)00480-2.

[37] A. Astolfi and R. Ortega, "Immersion and invariance: A new tool for stabilization and adaptive control of nonlinear systems," *IEEE Trans. Autom. Control*, vol. 48, no. 4, pp. 590–606, Apr. 2003, doi: 10.1109/TAC.2003.809820.

[38] B. Benlahbib, N. Bouarroudj, S. Mekhilef, D. Abdeldjalil, T. Abdelkrim, F. Bouchafaa, and A. Lakhdari, "Experimental investigation of power management and control of a PV/wind/fuel cell/battery hybrid energy system microgrid," *Int. J. Hydrogen Energy*, vol. 45, no. 53, pp. 29110–29122, Oct. 2020, doi: 10.1016/j.ijhydene.2020.07.251.

[39] H. Taghavifar and H. Taghavifar, "Adaptive robust control-based energy management of hybrid PV-battery systems with improved transient performance," *Int. J. Hydrogen Energy*, vol. 46, no. 10, pp. 7442–7453, Feb. 2021, doi: 10.1016/j.ijhydene.2020.11.243.

[40] S. Padhy and S. Panda, "Application of a simplified grey wolf optimization technique for adaptive fuzzy PID controller design for frequency regulation of a distributed power generation system," *Protection Control Modern Power Syst.*, vol. 6, no. 1, pp. 1–16, Dec. 2021, doi: 10.1186/s41601-021-00180-4.

[41] G. Kannayeram, N. B. Prakash, and R. Muniraj, "Intelligent hybrid controller for power flow management of PV/battery/FC/SC system in smart grid applications," *Int. J. Hydrogen Energy*, vol. 45, no. 41, pp. 21779–21795, Aug. 2020, doi: 10.1016/j.ijhydene.2020.05.149.

MOHAMMAD HOSEIN SABZALIAN was born in Iran. He received the Ph.D. degree in control science and engineering from Shanghai Jiao Tong University (SJTU), China. He is currently working as a Postdoctoral Researcher with the Laboratory of Power Electronics and Medium Voltage Applications (LEMT), Federal University of Rio de Janeiro (UFRJ), Rio de Janeiro, Brazil. His research interests include control theory, intelligent controllers, machine learning, fuzzy systems, adaptive control, nonlinear control, and their applications in several fields, including power systems automation, smart grids, mechanical systems, autonomous vehicles, and chaotic systems.

KHALID A. ALATTAS (Member, IEEE) received the B.Sc. degree in computer science from King Abdulaziz University, Saudi Arabia, the M.Sc. degree in telecommunication networks from New York University, NY, USA, and the M.Sc. and Ph.D. degrees in computer science from the University of Louisiana at Lafayette, USA. He is currently an Assistant Professor with the College of Computer Science and Engineering, University of Jeddah, Saudi Arabia. His research interests include networks, machine learning, data analytics, robotics, and unmanned vehicles. He serves as a reviewer for many international journals.

MAURICIO AREDES (Senior Member, IEEE) received the B.S. degree in electrical engineering from Universidade Federal Fluminense (UFF), in 1984, the master's degree from COPPE/UFRJ, in 1991, and the Ph.D. degree *(summa cum laude)* from Technische Universitaet Berlin (TUB), in 1996. In 1984, he was a Professor with UFF. From 1985 to 1988, he worked as a Commissioning Engineer at Itaipu HVDC Transmission System, and as a Management Assessor for the SCADA System Project of the Itaipu Power Plant. In the years of 1996 and 1997, he worked as a Researcher with the Electrical Energy Research Center (CEPEL). In 2006, he founded the Laboratory of Power Electronics and Medium Voltage Applications (LEMT), that enabled him to coordinate over 40 Research & Development projects at UFRJ. Since 1977, he has been a Professor with the Universidade Federal do Rio de Janeiro (UFRJ), associated with the Electrical Engineering Department, Escola Politécnica of the UFRJ and the Electrical Engineering Program from COPPE/UFRJ. He is the coauthor of a book, and has published more than 50 peer-reviewed journal articles and 180 in conference proceedings. His research interests include electric power systems, hybrid AC/DC power systems, smart grids, microgrids, renewable sources, and energy storage systems. From 2014 to 2018, he was a member of the Deliberative Council (CD) of COPPE (www.lemt.ufrj.br).

ABDULLAH K. ALANAZI received the M.Sc. degree from the Chemistry and Technology Department, University of New England (UNE), NSW, Australia, with thesis title related to (Nanotechnology and Heterogeneous Catalysis: Conversion of 2-Butanol to Butene Over MgO), in 2010, and the Ph.D. degree from UNE, in November 2016, with a thesis title:(Variable Kinetic Parameters for Catalytic Reactions of Isobutene Over Zeolites). He is currently an Associate Professor in transformation processes and nano-materials science. He has been an Associate Professor with the Department of Chemistry, Faculty of Science, Taif University, since 2018. He has 18 scientific papers in world-international scientific journals. His oral papers are presented at famous international conferences. He is a Senior Researcher in two projects funded by Taif University. His research interests include new energy and petroleum oil, preparation of green nano-materials, and their applications in the fields of sustainable energy and the environment.

HALA M. ABO-DIEF received the B.Sc. degree from the Chemical Engineering Department, Minia Faculty of Engineering, in 1996, the M.Sc. degree from the Chemical Engineering Department, Minia Faculty of Engineering, with a thesis title: "Kinetic Discussion for Some Metal Cementation Reaction," in 2003, and the Ph.D. degree from the Chemical Engineering Department, Minia Faculty of Engineering, with a thesis title: "Study on Corrosion Inhibition of Carbon Steel Samples in The Egyptian Petroleum Industry," in 2008. She worked as an Engineer with the Criminal Evidence Department, Ministry of Interior, El-Minia, Egypt, in 1997. She was a Research Assistant with the Petroleum Evaluation and Analysis Department, Petroleum Research Institute, in 2003. She was an Assistant Professor with the Petroleum Evaluation and Analysis Department, in 2008, Petroleum Research Institute, Nasr City, Cairo, Egypt, where she was an Associate Professor with the Petroleum Evaluation and Analysis Department, in 2015. She has been an Assistant Professor with The Chemistry Department, Faculty of Science, Al-Taif University, Saudi Arabia, since 2012. She is currently an Associate Professor in petroleum oil testing's and nano-materials science. She has 73 scientific papers at the famous world periodicals and conferences. Her papers are oral presented in 31 famous international conferences. She is a Senior Researcher in ten funded Projects from Al-Taif University and she is a Research Partner in 15 Projects funded from Al-Taif, AlQassiem, Umm Al-Querra and Al-Baha Universities. She shared in the evaluation of many projects for many universities and she is a reviewer of many international scientific journals.

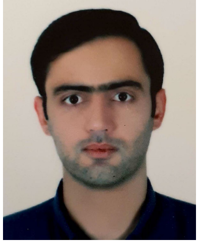

ARDASHIR MOHAMMADZADEH is currenty an Assistant Professor of Control Engineering with the Department of Electrical Engineering, University of Bonab. He also collaborates with Duy Tan University, Da Nang, Vietnam. He has published many papers in most reputed journals. His research interests include control theory, fuzzy logic systems, machine learning, neural networks, intelligent control, electrical vehicles, power systems control, chaotic systems, and medical systems. He is an Academic Editor of *Plos One* and a Reviewer of several journals, such as IEEE Transactions on Fuzzy Systems, *Applied Soft Computing*, *Nonlinear Dynamics*, and many others.

SALEH MOBAYEN (Senior Member, IEEE) is currently an Associate Professor of Control Engineering with the Department of Electrical Engineering, University of Zanjan. He also collaborates with the National Yunlin University of Science and Technology as an Associate Professor of the Future Technology Research Center. He has published several papers in the national and international journals. His research interests include control theory, sliding mode control, robust tracking, non-holonomic robots, and chaotic systems. He is a member of the IEEE Control Systems Society and serves as a member for program committee of several international conferences. He is an Associate Editor of *Artificial Intelligence Review*, *International Journal of Control, Automation and Systems*, *Circuits, Systems, and Signal Processing*, *Simulation*, *Measurement and Control*, and *International Journal of Dynamics and Control*. He is an Academic Editor of *Complexity* and *Mathematical Problems in Engineering*.

BRUNO WANDERLEY FRANÇA (Member, IEEE) received the B.Sc., M.Sc., and D.Sc. degrees in electrical engineering from the Federal University of Rio de Janeiro, Rio de Janeiro, Brazil, in 2009, 2012, and 2016, respectively. Since 2017, he has been an Associate Professor with the Department of Electrical Engineering, Fluminense Federal University (UFF), Rio de Janeiro. He is ahead of the Laboratory for Novel & Interdisciplinary Technologies in Electrical Engineering (NITEE), a Research Group founded, in 2018, of the Postgraduate Program in electrical and telecommunications engineering. His research interests include power electronics, distributed generation, microgrids and smart grids, power quality issues, renewable and energy storage systems, HVDC transmission, flexible AC transmission systems, and active filters.

AFEF FEKIH (Senior Member, IEEE) received the B.Sc., M.Sc., and Ph.D. degrees in electrical engineering from the National Engineering School of Tunis, Tunisia, in 1995, 1998, and 2002, respectively. She is currently a Full Professor with the Department of Electrical and Computer Engineering and a Chevron/BORSF Professor in engineering with the University of Louisiana at Lafayette, Lafayette, USA. She has authored or coauthored more than 200 publications in international journals, chapters, and conference proceedings. Her research interests include control theory and applications, including nonlinear and robust control, optimal control, fault tolerant control with applications to power systems, wind turbines, and unmanned vehicles and automotive engines. She is a member of the Editorial Board of IEEE Conference on Control Technology and Applications, IEEE Transactions on Education, and IFAC TC on *Power and Energy Systems*.